

Sticky PDMP samplers for sparse and local inference problems

Joris Bierkens ¹, Sebastiano Grazzi ¹,
Frank van der Meulen ¹, and Moritz Schauer ²

¹Delft Institute of Applied Mathematics (DIAM), Delft University of Technology

²Department of Mathematical Sciences, Chalmers University of Technology and University of Gothenburg

March 1, 2025

Abstract

We construct a new class of efficient Monte Carlo methods based on continuous-time piecewise deterministic Markov processes (PDMPs) suitable for inference in high dimensional sparse models, i.e. models for which there is prior knowledge that many coordinates are likely to be exactly 0. This is achieved with the fairly simple idea of endowing existing PDMP samplers with “sticky” coordinate axes, coordinate planes etc. Upon hitting those subspaces, an event is triggered during which the process *sticks* to the subspace, this way spending some time in a sub-model. This results in *non-reversible* jumps between different (sub-)models. While we show that PDMP samplers in general can be made sticky, we mainly focus on the Zig-Zag sampler. The computational efficiency of our method (and implementation) is established through numerical experiments where both the sample size and the dimension of the parameter space are large.

Keywords: Bayesian variable selection, piecewise deterministic Markov process, Monte Carlo, spike-and-slab, big-data, high-dimensional problems, non-reversible jump

1 Introduction

1.1 Overview

Consider the problem of simulating from a measure μ on \mathbb{R}^d that is a mixture of atomic and continuous components. A key application is Bayesian inference for sparse problems and variable selection under a spike-and-slab prior μ_0 of the form

$$\mu_0(dx) = \prod_{i=1}^d (w_i \pi_i(x_i) dx_i + (1 - w_i) \delta_0(dx_i)). \quad (1.1)$$

Here, $w_i \in [0, 1]$, $\pi_1, \pi_2, \dots, \pi_d$ are densities with respect to the Lebesgue measure referred to as *slabs* and δ_0 denotes the Dirac measure at zero. For sampling from μ , it is common to construct and simulate a Markov process with μ as invariant measure. State-of-the-art samplers such as the Hamiltonian Monte Carlo sampler (Duane et al., 1987) cannot be applied directly due to the degenerate nature of μ . We show that “ordinary” samplers based on piecewise deterministic Markov processes (PDMPs) can be adapted to sample from μ by introducing *stickiness*.

In piecewise deterministic Markov processes, the state space is augmented by adding to each coordinate x_i a velocity component v_i , doubling the dimension of the state space. They are characterized by

piecewise deterministic dynamics between event times, where event times correspond to changes of velocities. PDMPs have received recent attention because they have good mixing properties (they are non-reversible and have ‘momentum’, - Andrieu and Livingstone, 2019), they take gradient information into account and they are attractive in Bayesian inference scenarios with a large number of observations because they allow for subsampling of the observations without creating bias (Bierkens, Fearnhead, and Roberts, 2019, Bierkens et al., 2020).

We introduce “sticking event times”, which occur every time a coordinate of the process state hits 0. At such time that particular component of the state freezes for an independent exponentially distributed time with rate $|v_i|\kappa_i$, for some $\kappa_i > 0$. This corresponds to temporarily setting the marginal velocity to 0: the process “sticks to (or freezes at) 0” in that coordinate, while the other coordinates keep moving, as long as they are not stuck themselves. After the exponentially distributed time the coordinate moves again with its original velocity, see Figure 1 for an illustration. By this we mean that the dynamics of a ordinary PDMP are adjusted such that the process can spend a positive amount of time at the origin, at the coordinate axes and at the coordinate (hyper-)planes by sticking to 0 in each coordinate for a random time span whenever the process hits 0 in that particular coordinate. By restoring the original velocity of each coordinate after sticking at 0, we effectively generate *non-reversible jumps between states with different sets of non-zero coordinates*. In the Bayesian context this corresponds to having non-reversible jumps between models of varying dimensionality.

This allows us to construct a piecewise deterministic process that has a pre-specified measure μ as invariant measure, which we assume to be of the form

$$\mu(dx) = C_\mu \exp(-\Psi(x)) \prod_{i=1}^d \left(dx_i + \frac{1}{\kappa_i} \delta_0(dx_i) \right) \quad (1.2)$$

for some differentiable function Ψ , normalising constant $C_\mu > 0$ and positive parameters $\kappa_1, \kappa_2, \dots, \kappa_d$. Here the Dirac masses are located at 0, but generalizations are straightforward. The resulting samplers and processes are referred to as *sticky samplers* and *sticky piecewise deterministic Markov processes* respectively. The proportionality constant C_μ is assumed to be unknown while $(\kappa_i)_{i=1, \dots, d}$ are known. This is a natural assumption; suppose a statistical model with parameter x and log-likelihood $\ell(x)$ (notationally, we drop the dependence of ℓ on the data). Under the spike-and-slab prior defined in equation (1.1), the posterior measure is of the form of equation (1.2) with

$$\Psi(x) = C - \ell(x) - \sum_{i=1}^d \log(\pi_i(x_i)), \quad \kappa_i = \frac{w_i}{1 - w_i} \pi_i(0) \quad (1.3)$$

where C , independent of x , can be chosen freely for convenience. A popular choice for π_i is a Gaussian density centered at 0 with standard deviation σ_i . In this case, as $w/(1-w) \approx w$ for $w \approx 0$, κ_i depends linearly on w_i/σ_i in the sparse setting.

Relevant quantities useful for model selection, such as the posterior probability of a model excluding the first variable

$$\mu(\{0\} \times \mathbb{R}^{d-1}) = C_\mu \int \exp(-\Psi(x)) \frac{1}{\kappa_1} \delta_0(dx_1) \prod_{i=2}^d \left(dx_i + \frac{1}{\kappa_i} \delta_0(dx_i) \right)$$

cannot be directly computed if C_μ is unknown. However, given a trajectory $(x(t))_{0 \leq t \leq T}$ of a PDMP with invariant measure μ , the quantity $\mu(\{0\} \times \mathbb{R}^{d-1})$ can be approximated by the ratio T_0/T where $T_0 = \text{Leb}\{0 \leq t \leq T: x_1(t) = 0\}$. This simple, yet general idea requires the user only to specify $\{\kappa_i\}_{i=1}^d$ and Ψ according to the relations of equation (1.3). Moreover, the posterior probability that a collection of variables are all jointly equal to zero can be estimated in a similar way by computing the fraction of time that all corresponding coordinates of the process are simultaneously zero and, more generally, expectations of functionals with respect to the posterior can be estimated from the simulated trajectory.

In this article we focus on the sticky version of the Zig-Zag sampler (Bierkens, Fearnhead, and Roberts, 2019) which can exploit efficiently a sparse dependence structure between coordinates through a local

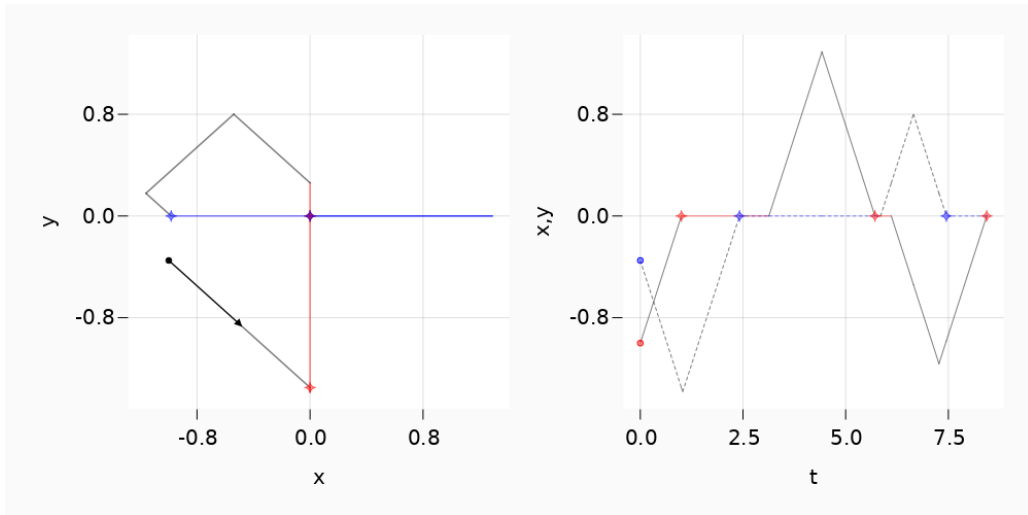


FIGURE 1: 2-dimensional Sticky Zig-Zag sampler with initial position $(-1.0, -0.4)$ and initial velocity $(+1, -1)$. On the left panel, a trajectory on the (x, y) -plane of the Sticky Zig-Zag sampler. The sticky event times relative to the x (respectively y) coordinate and the trajectories with the x (respectively y) stuck at 0 are marked with a blue (respectively red) cross and line. On the right panel, the trajectories of each coordinate against the time using the same (color-) scheme. The trajectory of y is dashed.

implementation (see Section 3). Appendix B extends the results for two other sticky samplers: the sticky version of the Bouncy particle sampler (Bouchard-Côté, Vollmer, and Doucet, 2018) and the Boomerang sampler (Bierkens et al., 2020), the latter having Hamiltonian deterministic dynamics invariant to a prescribed Gaussian measure. In Section 4 we analyze the performance of the algorithm and in Section 5 we apply our method in a number of examples. These results are compared with those obtained when using the Gibbs sampler for variable selection. The Julia package `ZigZagBoomerang.jl` (Schauer and Grazi, 2021) implements the sticky PDMP samplers from this article for general use.

1.2 Related literature

The main purpose of this paper is to show how “ordinary” PDMPs can be adjusted to sample from the measure μ as defined in (1.2). The numerical examples illustrate its applicability in a wide range of applications. One specific application that has received much attention in the statistical literature is variable selection using a spike-and-slab prior. For the linear model, early contributions include Mitchell and Beauchamp (1988) and George and McCulloch (1993). Some later contributions for hierarchical models derived from the linear model are Ishwaran and Rao (2005), Guan and Stephens (2011), Zanella and Roberts (2019) and Liang, Livingstone, and Griffin (2021). These works have in common that samples from the posterior are obtained from Gibbs sampling, where efficiency is achieved by exploiting the structure offered by specific models. A general and common framework for MCMC methods for variable selection was introduced in Green (1995) and Green and Hastie (2009) and referred to as *reversible jump MCMC*.

Methods that scale better (compared to Gibbs sampling) with either the sample size or dimension of the parameter can be obtained in different ways. Firstly, rather than sampling from the posterior one can *approximate* the posterior within a specified class, for example using variational inference. As an example, Ray, Szabo, and Clara (2020) adopt this approach in a logistic regression problem with spike-and-slab prior. Secondly, one can try to obtain sparsity using a prior which is not of spike-and-slab type. For example, Griffin and Brown (2021) consider Gibbs sampling algorithms for the linear model with priors that are designed to promote sparseness, such as the Laplace or horseshoe prior (on the parameter vector). While such methods scale well with dimension of data and parameter, these target a different problem: the posterior is not of the form (1.2). That is, the posterior itself is not sparse (though derived point estimates may be sparse and the posterior itself may have good properties

when viewed from a frequentist perspective). Moreover, part of the computational efficiency is related to the specific model considered (linear or logistic model) and, arguably, a generic gradient-based MCMC method would perform poorly on such measures since the gradient of the (log-)density near 0 in each coordinate explodes to account for the change of mass in the neighborhood of 0 induced by the continuous spike component of the prior.

Recent independent and parallel work by Chevallier, Fearnhead, and Sutton (2020) addresses variable selection problems using PDMP samplers. The approach taken in that paper is based on the framework of reversible jump MCMC as proposed in Green, 1995 and is therefore different from our approach. Nonetheless, the samplers have certain similarities. The dynamics of both the RJ PDMPs in Chevallier, Fearnhead, and Sutton (2020) and the sticky PDMPs proposed in this paper allow each coordinate to stick at 0 for an exponential time. The rate of the exponential time of the sticky PDMPs depends only on the velocity component of each coordinate, while the rate of RJ PDMPs can depend on the current state of the process. The latter is slightly more general as it allows to choose freely a prior weight on the Dirac measure for each possible model (while our approach allows to choose freely a prior weight on the Dirac measure of each possible coordinate). An important difference between the two methods is the behaviour of the process after the particle sticks at 0: the velocity of the coordinate of the sticky PDMPs is restored to its previous value while for RJ PDMPs, a new velocity is drawn independently to the previous one. The former action introduces non-reversible jumps between models while the latter reversible jumps and a random walk behaviour when jumping between models. For RJ PDMPs, this last effect is mitigated by introducing a tuning parameter p which allows each coordinate to stick at 0 only a fraction of times when hitting 0 (and compensating for this by down-scaling the rate of the exponential waiting time when the coordinate sticks). The parameter p is tuned to be equal to 0.6 based on empirical criteria. In Appendix C we investigate the possibility to introduce the tuning parameter p in the Sticky Zig-Zag sampler and, based on a heuristic argument and a simulation study, we concluded that it is not beneficial for us. Although for classical variable selection scenarios we expect the two approaches to perform similarly, in Appendix C further simulations are carried out which unveil different scaling limits of the Sticky Zig-Zag and the RJ Zig-Zag processes as the number of Dirac measures increases: while the Sticky Zig-Zag converges to ordinary Zig-Zag, the RJ Zig-Zag asymptotically exhibits diffusive behaviour.

2 Sticky PDMP samplers

2.1 General framework

The i th element of the vector $x \in \mathbb{R}^d$ is denoted by x_i . We denote $x_{-i} := (x_1, x_2, \dots, x_{i-1}, x_{i+1}, \dots, x_d) \in \mathbb{R}^{d-1}$. Write

$$(x[k: y])_i := \begin{cases} x_i & i \neq k, \\ y & i = k. \end{cases}$$

and $[x]_A := (x_i)_{i \in A} \in \mathbb{R}^{|A|}$ for a set of indexes $A \subset \{1, 2, \dots, d\}$ with cardinality $|A|$. We denote by \sqcup the disjoint union between sets and the positive and negative part of a real-valued function f by $f^+ := \max(0, f)$ and $f^- := \max(0, -f)$ respectively so that $f = f^+ - f^-$. For a topological space E , let $\mathcal{B}(E)$ denote the Borel σ -algebra on E . Denote by $\mathcal{M}(E)$ the class of Borel measurable functions $f: E \rightarrow \mathbb{R}$ and let $C(E) = \{f \in \mathcal{M}(E): f \text{ is continuous}\}$.

The state space of the the sticky PDMPs contains two copies of zero for each coordinate position. This construction allows a coordinate process arriving at zero from below (above) to spend an exponentially distributed time at zero before jumping to the “other” zero and continuing the dynamics. Formally, let $\overline{\mathbb{R}}$ be the disjoint union $\overline{\mathbb{R}} = (-\infty, 0^-] \sqcup [0^+, \infty)$ with the natural topology¹ τ , where we use the notation 0^- , 0^+ to distinguish the zero element in $(-\infty, 0]$ from the zero element in $[0, \infty)$. The

¹A function $f: \overline{\mathbb{R}} \rightarrow \mathbb{R}$ is continuous if both restrictions to $(-\infty, 0^-]$ and $[0^+, \infty)$ are continuous. If $f(0^-) = f(0^+)$, we write $f(0)$.

process has *càdlàg*² trajectories in the locally compact state space $E = \overline{\mathbb{R}}^d \times \mathcal{V}$, where $\mathcal{V} \subset \mathbb{R}^d$. Pairs of position and velocity will typically be denoted by $(x, v) \in \overline{\mathbb{R}}^d \times \mathcal{V}$. A trajectory reaching zero in a coordinate from below (with positive velocity) or from above (with negative velocity) spends time at the closed end of the half open interval $(-\infty, 0^-]$ ($[0^+, \infty)$). Thus the i th coordinate of the particle is sticking to zero (or frozen), if the particle's state is element of the i th frozen boundary $\mathfrak{F}_i \subset E$ given by

$$\mathfrak{F}_i = \{(x, v) \in E: x_i = 0^-, v_i > 0 \text{ or } x_i = 0^+, v_i < 0\}.$$

Sometimes, we abuse notation by writing $(x_i, v_i) \in \mathfrak{F}_i$ when $(x, v) \in \mathfrak{F}_i$ as the set \mathfrak{F}_i has restrictions only on x_i, v_i . The closed endpoints of the half-open intervals are somewhat reminiscent of sticky boundaries in the sense of Liggett (2010, Example 5.59). Denote by $\alpha \equiv \alpha(x, v)$ the set of indices of active coordinates, defined by

$$\alpha = \{i \in \{1, 2, \dots, d\}: (x, v) \notin \mathfrak{F}_i\} \quad (2.1)$$

and its complement $\alpha^C = \{1, 2, \dots, d\} \setminus \alpha$. Furthermore define a jump or *transfer mapping* $T_i: \mathfrak{F}_i \rightarrow E$ by

$$T_i(x, v) = \begin{cases} (x[i: 0^+], v) & \text{if } x_i = 0^-, v_i > 0, \\ (x[i: 0^-], v) & \text{if } x_i = 0^+, v_i < 0. \end{cases}$$

The sticky PDMPs on the space E are determined by their infinitesimal characteristics: their dynamics are determined by random state changes happening at random jump times of a time inhomogeneous Poisson process with intensity depending on the state of the process, and a deterministic flow governed by a differential equation in between. The state changes happen according to a Markov kernel $\mathcal{Q}: E \times \mathcal{B}(E) \rightarrow [0, \infty)$, at random times sampled with state dependent intensity $\lambda: E \rightarrow [0, \infty)$. The deterministic dynamics are determined by the integral equation

$$(x(t), v(t)) = (x(s), v(s)) + \int_s^t \xi(x(r), v(r)) dr, \quad (2.2)$$

with $\xi: E \rightarrow E$, which determines the operator $\mathfrak{X}f = \sum_i \xi_i^x \partial_{x_i} f + \sum_i \xi_i^v \partial_{v_i} f$, for $f \in C^1(E)$ where ξ^x and ξ^v denote the location and velocity component of ξ respectively.

Typically we think of different types of state changes given by Markov kernels $\mathcal{Q}_1, \mathcal{Q}_2, \dots$, for example refreshments, reflections, etc. If each transition is triggered by its individual independent Poisson clock with intensity $\lambda_1, \lambda_2, \dots$, then $\lambda = \sum_i \lambda_i$, and \mathcal{Q} itself can be written as the mixture

$$\mathcal{Q}((x, v), \cdot) = \sum_i \frac{\lambda_i((x, v))}{\lambda((x, v))} \mathcal{Q}_i((x, v), \cdot).$$

With that, the dynamics of the sticky PDMP sampler $t \mapsto (X(t), V(t))$ are as follows: starting from $(x, v) \in E$,

1. its flow in each coordinate is deterministic and continuous until an event happens. The deterministic dynamics are given by (2.2) componentwise for functions $\xi_i: \overline{\mathbb{R}} \times \mathbb{R} \rightarrow \overline{\mathbb{R}} \times \mathbb{R}$ which depend on the specific PDMP chosen (typically $\xi_i = \xi_j$ for all $i, j \in 1, \dots, d$). Upon hitting \mathfrak{F}_i , the i th coordinate process freezes, captured by the state dependence of (2.2).
2. A frozen coordinate “unfreezes” or “thaws” at rate equal to $\kappa_i |v_i|$ by jumping according to the transfer mapping T_i to the location $(0^+, v_i)$ respective $(0^-, v_i)$ outside \mathfrak{F}_i and continuing with the *same* velocity as before. That is, on hitting \mathfrak{F}_i , the i th coordinate process freezes for an independent exponentially distributed time with rate $\kappa_i |v_i|$. This constitutes a non-reversible move between models of different dimension. The corresponding transition $\mathcal{Q}_{i, \text{thaw}}$ is the Dirac measure at $\delta_{T_i(x, v)}$ and the intensity component $\lambda_{i, \text{thaw}}$ equals $\kappa_i |v_i| \mathbf{1}_{\mathfrak{F}_i}$.

²I.e., trajectories that are continuous from the right, with existing limits from the left.

3. An inhomogeneous Poisson process with rate depending on Ψ triggers the reflection events. At a reflection event time, the process changes its velocities according to its reflection rule in such a way that the process is invariant to the measure μ .
4. Refreshment events can be added, where, at exponentially distributed times, the velocity changes according to a refreshment rule leaving the measure μ invariant. Refreshments are sometimes necessary for the process to be ergodic.

A sample of the sticky PDMP is given by a recursive construction. Let $s \rightarrow \varphi(s, x, v)$ be the deterministic solution of (2.2) starting in (x, v) . Set $\tau_0 = 0$ and assume position and velocity vectors x and v at time 0. Given the current state $(X(\tau_i), V(\tau_i))$ at time τ_i ,

1. sample independently Δ_i as the first event time of an inhomogeneous Poisson process. We denote $\Delta_i \sim \text{Poiss}(s \rightarrow \lambda(\varphi(s, X(\tau_i), V(\tau_i))))$, with

$$P(\Delta_i \geq t) = \exp\left(-\int_0^t \lambda(\varphi(s, X(\tau_i), V(\tau_i))) ds\right). \quad (2.3)$$

2. Let $\tau_{i+1} = \tau_i + \Delta_i$ and set for $t \in [\tau_i, \tau_{i+1})$

$$(X(t), V(t)) = \varphi(t - \tau_i, X(\tau_i), V(\tau_i)).$$

3. Let

$$(X(\tau_{i+1}), V(\tau_{i+1})) \sim \mathcal{Q}(\varphi(\Delta_i, X(\tau_i), V(\tau_i)), \cdot).$$

The resulting stochastic process (X_t, V_t) is a sticky PDMP with dynamics \mathcal{Q} , λ , φ , initialised in (x, v) . Properties of this process can then be derived from \mathcal{Q} , λ and \mathfrak{X} and, in particular, with the operator

$$(\mathcal{A}f)(x, v) = (\mathfrak{X}f)(x, v) + \lambda(x, v) \int (f(x', v') - f(x, v)) \mathcal{Q}((x, v), d(x', v'))$$

for all functions $f \in \mathcal{D}(\mathcal{A})$ with

$$\mathcal{D}(\mathcal{A}) = \{f: \forall (x, v) \in E, f(X(t), V(t)) - f(x, v) + \int_0^t \mathcal{A}f(X(s), V(s)) ds \text{ are local martingales.}\}$$

as specified in Davis (1993, Section 24).

Most importantly, if μ is such that $\int \mathcal{A}f d\mu = 0$ for a large class of functions f , for example all $f \in \mathcal{D}(\mathcal{A})$ and the process is Feller, then μ is the invariant measure of the process $(X(t), V(t))$. Here, the operator \mathcal{A} extends the generator \mathcal{L} of the Markov process $(X(t), V(t))$, formally defined as

$$\mathcal{L}f(x, v) := \lim_{t \downarrow 0} \frac{\mathbb{E}[f(X(t), V(t)) \mid X_0 = x, V_0 = v] - f(x, v)}{t}$$

for continuous functions f for which this limit exists uniformly in x and is continuous (see Liggett, 2010, Section 3 for more details). In what follows, we focus our attention on the Sticky Zig-Zag sampler and defer to Appendix B the details of the Bouncy Particle sampler and the Boomerang samplers.

2.2 Sticky Zig-Zag sampler

A trajectory of the Sticky Zig-Zag sampler has piecewise constant velocity which is an element of the set $\mathcal{V} = \{v: |v_i| = a_i, \forall i \in \{1, 2, \dots, d\}\}$ for a fixed vector a . For each index i , the deterministic dynamics of equation (2.2) are determined by the function $\xi_i(x_i, v_i) = (v_i \mathbb{1}_{(x_i, v_i) \notin \tilde{\mathfrak{F}}_i}, 0)$. Here all

random events are *factorised* coordinate-wise. The reflection time for the i th coordinate is determined by the inhomogeneous rate

$$\lambda_i(x, v) = \mathbb{1}_{i \in \alpha(x, v)} \left((v_i \partial_i \Psi(x))^+ + \lambda_{0, i}(x) \right),$$

for non-negative functions $\lambda_{0, i}$ which, in our experiments, we set to 0, as, in general, the smaller are the rates the more efficient is the algorithm (see for example Andrieu and Livingstone, 2019, Section 5.4). At reflection time, the sign of the velocity component of the state is flipped: $(x_i, v_i) \rightarrow (x_i, -v_i)$. The formal construction of the d -dimensional Sticky Zig-Zag process is rather technical and relies on the theory of piecewise deterministic processes developed in Davis (1993) (see Appendix A for full details). Here we highlight the main results.

Recall $t \rightarrow \varphi(t, x, v)$ denotes the deterministic solution of (2.2) starting in (x, v) and τ is the natural topology on E introduced in Section 2. Define the operator \mathcal{A} with domain

$$\begin{aligned} \mathcal{D}(\mathcal{A}) = \{ & f \in \mathcal{M}(E); t \mapsto f(\varphi(t, x, v)) \text{ } \tau\text{-absolutely continuous } \forall (x, v); \\ & \forall i, \lim_{t \downarrow 0} f(x[i: 0^+ + t], \cdot) = f(x[i: 0^+], \cdot), \lim_{t \downarrow 0} f(x[i: 0^- - t], \cdot) = f(x[i: 0^-], \cdot) \} \end{aligned}$$

by $\mathcal{A}f(x, v) = \sum_{i=1}^d \mathcal{A}_i f(x, v)$ with

$$\mathcal{A}_i f(x, v) = \begin{cases} a_i \kappa_i (f(T_i(x, v)) - f(x, v)) & (x, v) \in \mathfrak{F}_i, \\ v_i \partial_{x_i} f(x, v) + \lambda_i(x, v) (f(x, v[i: -v_i]) - f(x, v)) & \text{else.} \end{cases}$$

Proposition 2.1. *The extended generator of the d -dimensional Sticky Zig-Zag process is given by \mathcal{A} with domain $\mathcal{D}(\mathcal{A})$.*

Proof. See Appendix A.4. □

Denote the space of compactly supported functions on E which are continuously differentiable in their first argument by $C_c^1(E)$. Define also $C_b(E) = \{f \in C(E) : f \text{ is bounded}\}$ and $D = \{f \in C_c^1(E), \mathcal{A}f \in C_b(E)\}$.

Proposition 2.2. *The operator \mathcal{A} restricted to D coincides with the generator of the ordinary Zig-Zag process:*

$$\begin{aligned} D = \bigcap_{i=1, \dots, d} \{ & f \in C_c^1(E) : v_i \kappa_i (f(T_i(x, v)) - f(x, v)) \\ & = v_i \partial_i f(x, v) + \lambda_i(x, v) (f(x, v[i: -v_i]) - f(x, v)), (x, v) \in \mathfrak{F}_i \}. \end{aligned}$$

For $f \in D$, $\mathcal{A}f = \mathcal{L}f$, where $\mathcal{L}f = \sum_{i=1}^d \mathcal{L}_i f$ with

$$\mathcal{L}_i f(x, v) = v_i \partial_{x_i} f(x, v) + \lambda_i(x, v) (f(x, v[i: -v_i]) - f(x, v)).$$

Theorem 2.3. *The d -dimensional Sticky Zig-Zag sampler is a Feller process and a strong Markov process in the topological space (E, τ) with unique invariant measure*

$$\mu(dx, dv) = \frac{1}{C} \sum_{u \in \mathcal{V}} \exp(-\Psi(x)) \prod_{i=1}^d \left(dx_i + \frac{1}{\kappa_i} (\mathbb{1}_{v_i > 0} \delta_{0^-}(dx_i) + \mathbb{1}_{v_i < 0} \delta_{0^+}(dx_i)) \delta_u(dv) \right), \quad (2.4)$$

for some normalization constant $C > 0$.

Proof. The construction of the process and the characterization of the extended generator and its domain of the d -dimensional Sticky Zig-Zag process can be found in Appendix A.1. We then prove that the process is Feller and strong Markov (Appendix A.2 and Appendix A.3). By Liggett (2010), Theorem 3.37, μ is the unique invariant measure if, for all $f \in D$, $\int \mathcal{L}f d\mu = 0$. This last equality is derived in Appendix A.5. □

2.3 Zig-Zag subsampling method

Here we address the problem of sampling a d -dimensional target measure when the log-likelihood is a sum of N terms, when d and N are large. Consider for example a regression problem where both the number of covariates and the number of experimental units in the dataset are large. In this situation the full evaluation of the log-likelihood and its gradient is prohibitive. However, PDMP samplers can still be used with the exact subsampling technique (e.g. Bierkens, Fearnhead, and Roberts, 2019) as this allows for substituting the gradient of the log-likelihood (which is required for deriving the reflection times) by an estimate of it which is cheaper to evaluate, without introducing any bias on the output of the sampler.

The subsampling technique for Sticky Zig-Zag samplers requires to find an unbiased estimate of the gradient of Ψ in (1.2). To that end, assume the following decomposition:

$$\partial_{x_i} \Psi(x) = \left(\sum_{j=1}^{N_i} S(x, i, j) \right), \quad \forall x \in \bar{\mathbb{R}}^d, i = 1, 2, \dots, d, \quad (2.5)$$

for some scalar valued function S . This assumption is satisfied when the likelihood is a product of factors, such as for likelihoods of (conditionally) independent observations.

For fixed (x, v) and $x^* \in \mathbb{R}^d$, for each $i \in \alpha(x, v)$ the random variable

$$N_i (S(x, i, J) - S(x^*, i, J)) + \partial_{x_i} \Psi(x^*), \quad J \sim \text{Unif}(\{1, 2, \dots, N_i\})$$

is an unbiased estimator for $\partial_{x_i} \Psi(x)$. Define the Poisson rates

$$\tilde{\lambda}_{i,j}(x, v) = (v_i N_i (S(x, i, j) - S(x^*, i, j)) + v_i \partial_{x_i} \Psi(x^*))^+$$

and, for each $i \in \alpha$, $t \geq 0$, the bounding rates $\bar{\lambda}_i(t, x, v) \geq \tilde{\lambda}_{i,j}(\varphi(t, x, v))$, $\forall j \in \{1, 2, \dots, N_i\}$. The Sticky Zig-Zag with subsampling has the following dynamics:

- the deterministic dynamics and the sticky events are identical to the ones of the Sticky Zig-Zag sampler presented in Section 2.2;
- a *proposed* reflection time equals $\min_{i \in \alpha(x, v)} \tau_i$, with $\{\tau_i\}_{i \in \alpha(x, v)}$ being independent inhomogeneous Poisson times with rates $s \rightarrow \bar{\lambda}_i(s, x, v)$;
- at the proposed reflection time τ triggered by the i th Poisson clock, the process reflects its velocity according to the rule $(x, v) \rightarrow (x, v[i, -v_i])$ with probability $\tilde{\lambda}_{i,J}(\varphi(\tau, x, v)) / \bar{\lambda}_i(\tau, x, v)$ where $J \sim \text{Unif}(\{1, 2, \dots, N_i\})$.

Proposition 2.4. *The Sticky Zig-Zag with subsampling preserves the measure in Equation (2.4) invariant.*

The proof of Proposition 2.4 follows with a similar argument made in the proof of Bierkens, Fearnhead, and Roberts (2019, Theorem 4.1). The number of computations required by the Sticky Zig-Zag with subsampling to compute the next event time with respect to the quantity N is $\mathcal{O}(1)$ (since $\partial_{x_i} \Psi(x^*)$ can be pre-computed). This advantage comes at the cost of introducing ‘shadow event times’, which are event times where the velocity component does not reflect. The advantage of using subsampling over the standard samplers have been empirically shown and informally argued for example in Bierkens, Fearnhead, and Roberts (2019, Section 5) and Bierkens et al. (2020, Section 3) in regimes where the Bernstein von-Mises theorem holds (large N) and when choosing x^* to be the mode of the smooth component of the posterior density.

3 Simulating sticky PDMPs

Sticky samplers can be implemented recursively by modifying appropriately the ordinary PDMP samplers so to include sticky events as introduced in Section 2. We discuss how to integrate local implementations of the algorithms to increase the sampler’s performance in case of a sparse dependence structure in the target measure and in case of local upper-bounding rates.

Although PDMPs have continuous trajectories, the algorithm computes and saves only a finite collection of points (which we refer to as the skeleton of the continuous trajectory) corresponding to the positions, velocities and times where the deterministic dynamics of the process change. In between those points, the continuous trajectory can be deterministically interpolated.

In case the i th partial derivative of the negative score function is a sum of N_i terms, which is the case for example in regression problems, subsampling techniques can be employed as described in Section 2.3.

3.1 Computing Poisson times for PDMPs

As PDMPs move deterministically (and with simple dynamics) in between event times, the main computational challenge consists of simulating those times. Given an initial position (x, v) , the distribution of the time until the next event is specified in (2.3). A sample from this distribution can be found by solving for τ' in the equation

$$\int_0^{\tau'} \lambda(\varphi(s, x, v)) ds = t, \quad t = \text{Exp}(1). \quad (3.1)$$

We then write that $\tau' \sim \text{Poiss}(\lambda(\varphi(\cdot, x, v)))$. When it is not possible to find the root of equation (3.1) in closed form, it suffices to find upper bounds $\bar{\lambda}$ for the rate functions which satisfies, for any $(x, v) \in E$ and for some $\Delta = \Delta(x, v) > 0$

$$\bar{\lambda}(t, x, v) \geq \lambda(\varphi(t, x, v)), \quad \Delta \geq t \geq 0, \quad (3.2)$$

for which this is possible and use the thinning scheme: Let $\tau' \sim \text{Poiss}(\bar{\lambda}(\cdot, x, v))$; if $\tau' > \Delta$ then the proposed time is rejected and a new time has to be drawn as $\tau' \sim \text{Poiss}(\bar{\lambda}(\cdot, \phi(\Delta, x, v)))$. We *accept* the proposed time with probability $\lambda(\phi(\tau', x, v))/\bar{\lambda}(\tau', x, v)$. This scheme is referred as *adaptive thinning* in Bouchard-Côté, Vollmer, and Doucet (2018). More sophisticated and potentially efficient thinning schemes have been proposed, see Sutton and Fearnhead (2021). The simulation of unfreezing times is easier: once the i -th component hits zero then it sticks at zero for a time that is exponentially distributed with parameter $\kappa_i |v_i|$.

For the ordinary d -dimensional Zig-Zag and the factorised Boomerang sampler (these samplers are called *factorised PDMPs* in Bierkens et al., 2020), the reflection time is factorised as the minimum of d independent clocks $\tau_1, \tau_2, \dots, \tau_d$ where $\tau_i \sim \text{Poiss}(\lambda_i(\varphi(\cdot, x, v)))$. for $i = 1, 2, \dots, d$. The first reflection time of the d -dimensional sticky factorised samplers is obtained instead by finding the minimum of $|\alpha| < d$ independent clocks with the same rates λ_i of the ordinary factorised sampler, but only for the active coordinates $i \in \alpha(x, v)$.

If $\partial_{x_i} \Psi$ (an estimate of $\partial_{x_i} \Psi$ when using subsampling) or the upper bound $\bar{\lambda}$ depends on fewer coordinates, then the evaluation of each reflection time is cheaper. The fully local implementation presented in Bierkens et al. (2021) exploits these two features once in proposing the reflection time and once for deciding whether to accept. Below, we discuss in more details the algorithm of Sticky Zig-Zag sampler with local upper-bounds and with subsampling.

3.2 The local Sticky Zig-Zag

Local implementation: Assume that the sets \bar{A}_i and $\bar{\lambda}_i$ are such that

$$\bar{\lambda}_i(t, x, v) = f_i(t, x_{\bar{A}_i}), \quad \forall x, \text{ for } i = 1, 2, \dots, d$$

for some $f_i: \mathbb{R}^+ \times \mathbb{R}^{|\bar{A}_i|} \rightarrow \mathbb{R}^+$ with $\bar{A}_i \subset \{1, 2, \dots, d\}$. Given an initial position (x, v) and random times $\tau_j \sim \text{Pois}(t \rightarrow \bar{\lambda}_j(t, x, v))$, for $i \in \alpha$, denote by $i = \text{argmin}_{j \in \alpha(x, v)}(\tau_j)$ and $\tau = \min_{j \in \alpha(x, v)}(\tau_j)$ the first proposed reflection time. According to the thinning procedure for Poisson processes, the process flips the i th coordinate with probability $\lambda_i(\varphi(\tau, x, v)) / \bar{\lambda}_i(\tau, x, v)$. If the process flips the i th velocity, then the Poisson rates $\{\bar{\lambda}_j: j \in \alpha, \bar{A}_j \not\ni i\}$ continue to be valid upper bounds so that the corresponding reflection times do not need to be renewed (see Bierkens et al., 2021, Section 4, for implementation details).

In general, when the i th particle freezes at 0 or was stuck at 0 and gets released, the reflection times $\tau_j: i \in \bar{A}_j$ have to be renewed. However this is not always the case, as there are applications, such as the one in Section 5.4, for which the upper-bounding rates $\{\bar{\lambda}_i\}_{i=1}^d$ continue to be valid upper bounds when one or more particles hit 0 and therefore the waiting times computed before the particles hit 0 are still valid.

Fully local implementation: Consider now the decomposition of $\partial_{x_i}\Psi$, $i = 1, 2, \dots, d$ given in equation (2.5) and such that

$$S(x, i, j) = f_{i,j}(x_{\tilde{A}_{i,j}}), \quad \forall x, \text{ for } (i, j) \in \{1, 2, \dots, d\} \times \{1, 2, \dots, N_i\}$$

for some $f_{i,j}: \mathbb{R}^{|\tilde{A}_{i,j}|} \rightarrow \mathbb{R}$ with $\tilde{A}_{i,j} \subset \{1, 2, \dots, d\}$.

The fully local implementation of the Sticky Zig-Zag with subsampling profits from local upper bounds and local gradient estimators by assigning an independent time for each coordinate, thus evolving the flow of only the coordinates which are required at each step and by stacking all the reflection times $\tau_j: j \in \alpha$, the hitting times τ_j^* : $j \in \alpha$ and the unfreezing times $\tau_j^\circ: j \in \alpha^c$ in an ordered queue. For a documented implementation, see Schauer and Grazzi (2021).

Given an initial point (x, v) and if i is the coordinate of the first proposed reflection time $\tau_i = \min(\tau_j: j \in \alpha(x, v))$, the sampler reflects the velocity of the i th coordinate with probability $\tilde{\lambda}_{i,J}(x_{\tilde{A}_i}(t), v) / \bar{\lambda}(t, x, v)$ with $J \sim \text{Unif}(\{1, 2, \dots, N_i\})$. Hence, it is only required to update the position of the coordinates with index in $\tilde{A}_{i,J} \setminus \alpha^c(x, v)$. Then,

- if the i th velocity flips, then the algorithm needs to update only the waiting times $\{\tau_j: j \in \alpha, \bar{A}_j \ni i\}$ (as described in Subsection 3.2) and, to this end, needs to update the position of the coordinates with index $\{k \in \bar{A}_j \setminus \alpha^c(x, v): i \in \bar{A}_j\}$;
- in the other case, when the i th velocity does not change (shadow event), only τ_i has to be renewed so that only the particles in \bar{A}_i have to be updated.

Remark 3.1. (Sparse implementation.) When the dimensionality d is large, inserting each waiting time in a ordered queue and initializing the state space can be computationally expensive. If for example the product $k_i|v_i|$ is equal for all i , an alternative efficient and sparse implementation is possible. Here we simulate the sticky time for each frozen coordinate by means of simulating the overall sticky time from the exponential distribution with rate $\sum_{i \in \alpha^c} \kappa_i|v_i|$ (which has to be renewed every time a new particle sticks at 0) and selecting the particle to unfreeze uniformly from the set α^c . A further improvement can be obtained by representing x as a sparse vector and saving only the location of the active particles $\{x_i: i \in \alpha\}$.

4 Runtime analysis and comparisons for Gaussian models

In this section we discuss the performance of the Sticky Zig-Zag sampler in comparison with a popular method for variable selection based on Gibbs sampling. The comparison is primarily in relation to the dimension d , average number of active particles, weights $\{\kappa_i\}_{i=1,2,\dots,d}$ and sample size N of the problem. To make sensible comparisons, we focus on the case where Ψ in (1.2) admits the form $\Psi(x) = (x - \mu)' \Gamma (x - \mu)$ for $\mu \in \mathbb{R}^d$ and positive definite $\Gamma \in \mathbb{R}^{d \times d}$. We describe an extension of the Gibbs samplers presented in Chipman et al. (2001) that targets measures of this form. The analysis of both the Gibbs sampler and the Sticky Zig-Zag sampler takes into account that Γ can be sparse, which is the case for models with sparse conditional dependence structure between coordinates.

4.1 Gibbs samplers

Methods based on the Gibbs sampler for variable selection can be adopted only when it is possible to compute in closed form the Bayes factors, i.e. the ratio between posterior probabilities of different (sub-)models. We can use a set of active indices α to define a model, as the corresponding set of non-zero values in \mathbb{R}^d :

$$\mathcal{M}_\alpha := \{x \in \mathbb{R}^d : x_i = 0, i \in \alpha^c\} \quad \text{for } \alpha \subset \{1, 2, \dots, d\}.$$

For every set of indexes $\alpha \subset \{1, 2, \dots, d\}$ and for every j , the Bayes factors relative to two neighbouring (sub-)models (those differing by only one coefficient) for a measure as in equation (1.2) are given by

$$B_j(\alpha) = \frac{\mu(\mathcal{M}_{\alpha \cup \{j\}})}{\mu(\mathcal{M}_{\alpha \setminus \{j\}})} = \frac{\kappa_j \int_{\mathbb{R}^{\alpha \cup \{j\}}} \exp(-\Psi(y)) dx_{\alpha \cup \{j\}}}{\int_{\mathbb{R}^{\alpha \setminus \{j\}}} \exp(-\Psi(z)) dx_{\alpha \setminus \{j\}}}, \quad (4.1)$$

where $y = \{x \in \mathbb{R}^d : x_i = 0, i \notin (\alpha \cup \{j\})\}$, $z = \{x \in \mathbb{R}^d : x_i = 0, i \notin (\alpha \setminus \{j\})\}$. The Gibbs sampler starting in (x, α) , with $x_i \neq 0$ only if $i \in \alpha$ for some set of indexes $\alpha \subset \{1, 2, \dots, d\}$, iterates the following two steps:

1. Update α by choosing randomly $j \sim \text{Unif}(\{1, 2, \dots, d\})$ and set $\alpha \leftarrow \alpha \cup \{j\}$ with probability p_j where p_j satisfies $p_j/(1 - p_j) = B_j(\alpha)$, otherwise set $\alpha \leftarrow \alpha \setminus \{j\}$.
2. Update the free coefficients x_α according to the marginal probability of x_α conditioned on $x_i = 0$ for all $i \in \alpha^c$.

In Appendix D.1, we give an analytical expressions for the right hand-side of equation (4.1) and the posterior probability of step 2 when Ψ is a quadratic function of x . For logistic regression models, neither step 1 nor step 2 can be directly derived and the Gibbs samplers makes use of a further auxiliary Pólya-Gamma random variable ω which has to be simulated at every iteration and makes the computations of step 1 and step 2 tractable, conditionally on ω (see Polson, Scott, and Windle, 2013 for details).

4.2 Runtimes of the algorithms

We will now compute typical runtimes for the Gaussian model, assuming a decomposition

$$\Psi(x) = (x - \mu)' \Gamma (x - \mu) = \sum_{i=1}^N (x - \mu_i)' \Gamma_i (x - \mu_i) + c,$$

so that N captures the dependence on the number of observations in a Bayesian setting.

Sticky Zig-Zag sampler: The computational cost of simulating PDMP samplers is intimately related with the number of random times generated. This, in turn, depends on the intensity of the rate λ of

the underlying Poisson process. For any initial position and velocity (x, v) , the total rate of the Sticky Zig-Zag sampler is equal to

$$\lambda(x, v) = \sum_{i \in \alpha} \lambda_i(x, v) + \sum_{i \in \alpha^c} |v_i| \kappa_i \quad (4.2)$$

where, as before, $\alpha = \{i: x_i \neq 0\}$. In the following analysis, we drop the dependence on (x, v) and we assume that the size of $\alpha(t) := \{i: x_i(t) \neq 0\}$ fluctuates around a typical value p in stationarity. Thus p represents the number of non-zero components in a typical model, and can be much smaller than d in sparse models.

We consider the sticky Zig-Zag with local implementation as in Remark 3.1 where we assume $\kappa := \kappa_1 = \kappa_2 = \dots = \kappa_d$. We ignore logarithmic factors, e.g., for priority queue insertion. In the analysis below we distinguish between the computational costs of reflection events and unfreezing events.

The number of reflection and unfreezing events per unit time interval are respectively $\mathcal{O}(p)$ and $\mathcal{O}((d-p)\kappa)$ per unit time; see (4.2). Once either a reflection or unfreezing event happens, we have to recompute between $\mathcal{O}(1)$ and $\mathcal{O}(p)$ new reflection event times (depending on the elements of $\bar{A}_i \cap \alpha$; see Section 3). Finally, each newly computed reflection event time for the particles $i \in \alpha$ requires a computation ranging from $\mathcal{O}(1)$ to $\mathcal{O}(N)$. The complexity $\mathcal{O}(1)$ can be achieved using the subsampling technique (Section 2.3) in ideal scenarios (Bierkens, Fearnhead, and Roberts, 2019). Table 1 summarizes the overall scaling complexity of the Sticky Zig-Zag algorithm for the quantities p and N .

Gibbs sampler: At each iteration, the Gibbs sampler algorithm requires the evaluation of the Bayes factors which involves the inversion of a square matrix of dimension $p \times p$. This can be efficiently obtained with a Cholesky decomposition of a sub-matrix of Γ . This is a computation of $\mathcal{O}(p^3)$ when Γ is full; a lower order is possible when Γ is sparse. For example, in the example in Section 5.2, the complexity of this operation is $\mathcal{O}(p^{3/2})$. This is followed by computing sufficient statistics in step 2 of Section 4.1 which involves the inversion of a triangular matrix which is $\mathcal{O}(|\alpha^2|)$ ($\mathcal{O}(1)$ if the Cholesky factor is sparse) in addition to an operation of order pN (for example in linear or logistic regression). It is important to notice that if Γ is sparse, its Cholesky factors might not be. Our findings are summarized in Table 1 and validated by the numerical experiments of Section 5 (Figure 5, Figure 9).

Algorithm	Worst case	Best case
Sticky Zig-Zag	$p^2 N$	p
Gibbs sampler	$p(p^2 + N)$	$p(\sqrt{p} + N)$

TABLE 1: Computational scaling of the Sticky Zig-Zag algorithm and the Gibbs sampler for variable selection for p and sample size N . Worst case is when the target density does not present any conditional independence structure and the subsampling method for the Sticky Zig-Zag cannot be employed; best case when the target measure presents a relevant conditional independence structure and subsampling can be employed.

4.3 Mixing

Next to the complexity per iteration, we should also understand the number of iterations required to obtain an approximately independent sample. Given the different nature of dependencies of the two algorithms, a rigorous and theoretical comparison of their mixing times is difficult. We therefore provide a heuristic argument for two specific scenarios.

Let both algorithms be initialized at $x \sim \mathcal{N}_d(0, I)$ with all non-zero coordinates ($\alpha^c = \emptyset$) and assume that the target μ assigns most of its probability mass to the null model \mathcal{M}_\emptyset . Consider the following scenarios:

- A measure supported in every model and such that for any two models \mathcal{M}_{α_i} and \mathcal{M}_{α_j} with $\alpha_i \neq \alpha_j$, we have $\mu(\mathcal{M}_{\alpha_i}) > \mu(\mathcal{M}_{\alpha_j})$ if $|\alpha_i| < |\alpha_j|$, and approximately 0 otherwise. The Sticky Zig-Zag will be directed to the null model, each coordinate with speed 1, so that the first visit of the null set happens with an expected time $\mathcal{O}(\max_i(|x_i|))$ which is of $\mathcal{O}(\log d)$ if x is standard Gaussian. On the other hand, the Gibbs sampler, at every iteration, randomly picks a coordinate and, if this is a non-zero coordinate, succeeds to set that coordinate to zero. Denote by τ_α the (random) number of iterations needed for the algorithm to set any non-zero coordinate to zero, when exploring a model \mathcal{M}_α . Then $\mathbb{E}(\tau_\alpha) = d/|\alpha|$ which ranges from 1 (when \mathcal{M}_α is the full model) to d (for any sub-model with only one non-zero coordinate). Consider any sequence $\mathcal{M}_{\alpha_1}, \mathcal{M}_{\alpha_2}, \dots, \mathcal{M}_{\alpha_{d-1}}$ of models with $|\alpha_j| + 1 = |\alpha_{j+1}|$ (decreasing size) and with \mathcal{M}_{α_1} begin the full model. By adding the expected number of iterations at each of those model, we conclude that the process started at x in the full model, is expected to reach the null model in $\sum_{i=1}^d d/i$ iterations which is of $\mathcal{O}(d \log(d))$.
- A measure supported on a single nested sequence of sub-models, up to the full model: i.e. for a model \mathcal{M}_{α_j} , with $\mu(\mathcal{M}_{\alpha_j}) \neq 0$ there is only one sub-model $\mathcal{M}_{\alpha_i} \subset \mathcal{M}_{\alpha_j}$ with $|\alpha_i| + 1 = |\alpha_j|$ and the smaller model again has more probability mass $\mu(\mathcal{M}_{\alpha_i}) > \mu(\mathcal{M}_{\alpha_j})$. By a similar argument as above, the first expected visit time of the null model is of $\mathcal{O}(\sum_{i=1}^d |x_i|) = \mathcal{O}(d)$ for the Sticky Zig-Zag, while for the Gibbs sampler the expected number of steps is d^2 .

Table 2 summarizes the scaling results derived in the two cases considered above. Another interesting (and less extreme) scenario is considered in Section 5.3 where the posterior measure has modes on non-neighbouring sub-models. In this case the Gibbs sampler, by proposing models differing by only one variable at every iteration, is not able to explore the state space efficiently, while the Sticky Zig-Zag can mix fast as seen in the experiment of Section 5.3.

Algorithm	μ supported in every model	μ supported on a nested sequence
Sticky Zig-Zag	$\log(d)$	d
Gibbs sampler	$d \log(d)$	d^2

TABLE 2: Scaling relative to the dimension d of the expected time (number of iteration for the Gibbs sampler) to travel from the full model (initialized as a standard Gaussian random variable) to the null model (which is the mode of the target). The results are for targets which are supported in every model and for targets supported on a single sequence of nested sub-models.

Due to its continuous dynamics, the Sticky Zig-Zag can experience difficulty traversing regions of low density, in particular it will have difficulty reaching 0 in a coordinate if that requires passing through such a region. The following remark establishes a formula for the recurrence time of the Sticky Zig-Zag to the null model, and may serve as guidance in design of the probabilistic model or the choice of the parameter κ .

Remark 4.1. (Recurrence time of the Sticky Zig-Zag to zero.) The expected time to leave the null model for a d -dimensional Sticky Zig-Zag with unit velocity components is $\frac{1}{\kappa d}$ (since each coordinate leaves 0 according to an exponential random variable with parameter κ). A simple computation gives that the expected time of the process to return to the null model is

$$\frac{1 - \mu(\mathcal{M}_\emptyset)}{d\kappa\mu(\mathcal{M}_\emptyset)}. \quad (4.3)$$

5 Examples

In this section we apply the Sticky Zig-Zag sampler and, when possible, compare its performance with the Gibbs sampler in five different problems of varying nature and difficulty.

- A system of interacting agents where the dynamics of each agent are given by a stochastic differential equation. We aim to infer the interactions among agents. This is an example where the likelihood does not factorise and the number of parameters increases quadratically with the number of agents. We demonstrate the Sticky Zig-Zag sampler under a spike-and-slab prior on the parameters that govern the interaction and compare this with the Gibbs sampler.
- An image denoising problem where the prior incorporates that a large part of the image is black (corresponding to sparsity), but also promotes positive correlation among neighbouring pixels. Specifically, this examples illustrates that the Sticky Zig-Zag sampler can be employed in high dimensional regimes (the showcase is in dimension one million) and for sparsity promoting priors other than factorised priors such as spike-and-slab priors.
- A multi-modal model based on Gaussian increments of an unknown parameter; this is a constructed example where the Gibbs sampler fails to mix while the Sticky Zig-Zag sampler mixes well.
- The logistic regression model where both the number of covariates and the sample size are large, while assuming the coefficient vector to be sparse. This is a non-Gaussian optimal scenario where the Sticky Zig-Zag sampler can be employed with subsampling technique achieving $\mathcal{O}(1)$ scaling with respect to the sample size.
- The setting where N realisations of independent Gaussian vectors with precision matrix of the form XX' are observed. Sparsity is assumed on the off-diagonal elements of the lower-triangular matrix X . What makes this example particularly interesting is that the gradient of the log-likelihood explodes in some hyper-planes, complicating the application of gradient-based Markov chain Monte Carlo methods.

In all cases we simulate data from the model and assume the parameter to be sparse (i.e. most of its elements are assumed to be zero) and high dimensional. In case a spike-and-slab prior is used, the slabs are always chosen to be zero-mean Gaussian with (large) variance σ_0^2 . The sample sizes, parameter dimensions and additional difficulties such as correlated parameters or non-linearities which are considered in this section illustrate the computational efficiency of our method (and implementation) in a wide range of settings. In all examples we used the fully local algorithm of the Sticky Zig-Zag as detailed in Section 3.2 with velocities in the set $\mathcal{V} = \{-1, +1\}^d$. Comparisons with the Gibbs sampler are possible for Gaussian models and the logistic regression model. Our implementation of the Gibbs sampler is taking advantage of model sparsity as we have described in Section 4.1. Because of its computational overhead, when such comparisons are included, the dimensionality of the problems considered has been reduced. The performance of the two algorithms is compared by running the two algorithms for approximately the same computing time. As performance measure we consider the function

$$c \rightarrow \mathcal{P}_s(c) := \sum_{i=1}^d (p_i^s(c) - \bar{p}_i)^2,$$

where c denotes computing time (we use c rather than t as the latter is used as time index for the Zig-Zag sampler). In the displayed expression, we first compute \bar{p}_i , which is an approximation to the posterior probability of the i th coordinate being nonzero. This quantity can either be obtained by running the Sticky Zig-Zag sampler or the Gibbs sampler (if applicable) for a very long time. As we show the Sticky Zig-Zag sampler to converge faster, especially in high dimensional problems, we use this sampler in approximating this value. We stress that the same result could be obtained by running the Gibbs sampler for a very long time. More precisely, for each coordinate we compute for each coordinate of the Sticky Zig-Zag sampler the fraction of time it is nonzero. In $\mathcal{P}_s(c)$, the value of \bar{p}_i is compared to $p_i^s(c)$ which is the fraction of time (or fraction of samples in case of the Gibbs sampler) where x_i is nonzero using computational budget c and sampler ‘s’. All the experiments were carried out with a conventional laptop with Intel core i5-10310 processor and 16GB DDR4 RAM.

5.1 Learning networks of stochastic differential equations.

In this example we consider a stochastic model for p autonomously moving agents (“boids”) in the plane. The dynamics of the location of the i th agent is assumed to satisfy the stochastic differential equation

$$dU_i(t) = -\lambda U_i(t)dt + \sum_{j \neq i} x_{i,j}(U_j(t) - U_i(t))dt + \sigma dW_i(t), \quad 1 \leq i \leq p \quad (5.1)$$

where, for each i , $W_i(t)$ is an independent 2-dimensional Wiener process. We assume the trajectory of each agent is observed continuously over a fixed interval $[0, T]$. This implies $\sigma > 0$ can be considered known, as it can be recovered without error from the quadratic variation of the observed path. For simplicity we will also assume the mean-reversion parameter $\lambda > 0$ to be known. Let $x = \{x_{i,j} : i \neq j\} \in \mathbb{R}^{p^2-p}$ denote the unknown parameter. If $x_{i,j} > 0$, agent i has the tendency to follow agent j , on the other hand, if $x_{i,j} < 0$, agent i tends to avoid agent j . Hence, estimation of x aims at inferring which agent follows/avoids other agents. We will study this problem from a Bayesian point of view assuming sparsity of x , incorporated via the prior using a spike and slab prior. This problem has been studied previously in Bento, Ibrahimi, and Montanari (2010) using ℓ_1 -regularised least squares estimation.

Motivation for studying this problem can be found in Reynolds (1987) and the presentation at JuliaCon 2020 by Jesse Bettencourt (2020). An animation of the trajectories of the agents in time can be found at Grazi and Schauer (2021).

Suppose $U_i(t) = (U_{i,1}(t), U_{i,2}(t))$ and let $Y(t) = (U_{1,1}(t), \dots, U_{p,1}(t), U_{1,2}(t), \dots, U_{p,2}(t))$ denote the vector obtained upon concatenation of all x -coordinates and y -coordinates of all agents. Then, it follows from Equation (5.1) that $dY(t) = C(x)Y(t)dt + \sigma dW(t)$, where $W(t)$ is a Wiener process in \mathbb{R}^{2p} . Here, $C(x) = \text{diag}(A(x), A(x))$ where

$$A(x) = \begin{bmatrix} -\lambda - \bar{x}_1 & x_{1,2} & x_{1,3} & \dots \\ x_{2,1} & -\lambda - \bar{x}_2 & x_{2,3} & \\ x_{3,1} & & \ddots & \\ \vdots & & & \end{bmatrix}$$

with $\bar{x}_i = \sum_{j \neq i} x_{i,j}$. If \mathbb{P}_x denotes the measure on path space of $Y_T := (Y(t), t \in [0, T])$ and \mathbb{P}_0 denotes the Wiener-measure on \mathbb{R}^{2p} , then it follows from Girsanov’s theorem that

$$\ell(x) := \log \frac{\mathbb{P}_x}{\mathbb{P}_0}(Y_T) = \frac{1}{\sigma^2} \int_0^T (C(x)Y(t))' dY(t) - \frac{1}{2\sigma^2} \int_0^T \|C(x)Y(t)\|^2 dt. \quad (5.2)$$

As we will numerically only be able to store the observed sample path on a fine grid, we approximate the integrals appearing in the log-likelihood $\ell(x)$ using a standard Riemann-sum approximation of Itô integrals (see e.g. Rogers and Williams, 2000a, Ch. IV, sec. 47) and time integrals. We assume x to be sparse which is incorporated by choosing a spike-and-slab prior for x as in Equation (1.1). The posterior measure is of the form of (1.2) with κ and $\Psi(x)$ as in (1.3). As $x \mapsto \Psi(x)$ is quadratic, the reflection times of the Sticky Zig-Zag sampler can be computed in closed form.

Numerical experiments: In our numerical experiments we fix $p = 50$ (number of agents), $T = 200$ (length of time-interval), $\sigma = 0.1$ (noise-level) and $\lambda = 0.2$ (mean-reversion coefficient). We set the parameter x such that each agent has one agent that tends to follow and one agent that tends to avoid. Hence, for every i , we set $x_{i,j}$ to be zero for all $j \neq i$, except for 2 distinct indices $j_1, j_2 \sim \text{Unif}(\{1, 2, \dots, d\} \setminus i)$ with $x_{i,j_1} x_{i,j_2} < 0$. The parameter x is very sparse and it is highly nontrivial to recover its value. We then simulate Y_T using Euler forward discretization scheme, with step-size equal to 0.1 and initial configuration $Y(0) \sim \mathcal{N}_{2p}(0, I)$.

The prior weights $w_1 = w_2 = \dots = w_d$ (w_i being the prior probability of the i th coordinate to be nonzero) are conveniently chosen to equal the proportion of non-zero elements in the true (data-generating) parameter vector x . The variance of each slab was taken to be $\sigma_0^2 = 50$. We ran the Sticky

Zig-Zag sampler with final clock 500, where the algorithm was initialized in the full-model with no coordinate frozen at 0 at the posterior mean of the Gaussian density proportional to Ψ .

Figure 2 shows the discrepancy between the parameters used during simulation (ground truth) and the estimated posterior median. In this figure, from the (sticky) Zig-Zag trajectory of each element $x_{i,j}$ ($i \neq j$) we collected their values at time $t_i = i0.1$ and subsequently computed the median of the those values. We conclude that all parameters which are strictly positive (coloured in pink) are recovered well. At the bottom of the figure (black points and crosses), 25 are incorrectly identified as either being zero or negative. In this experiment, the Sticky Zig-Zag sampler outperforms the Gibbs sampler considerably.

In Figure 3 we compare the performance of the Sticky Zig-Zag sampler with the Gibbs sampler. Here, all the parameters (including initialisation) are as above, except now the number of agents is taken as $p = 20$. Both $c \rightarrow \mathcal{P}_{\text{Zig-Zag}}(c)$ and $t \rightarrow \mathcal{P}_{\text{Gibbs}}(c)$, with c denoting the computational budget, are computed for $c \in [0, 10]$. For this, the final clock of the Zig-Zag was set to 10^4 and the number of iterations for the Gibbs sampler was set to 1.2×10^4 . For obtaining \bar{p}_i the Sticky Zig-Zag sampler was run with final clock 5×10^4 (taking approximately 50 seconds computing time).

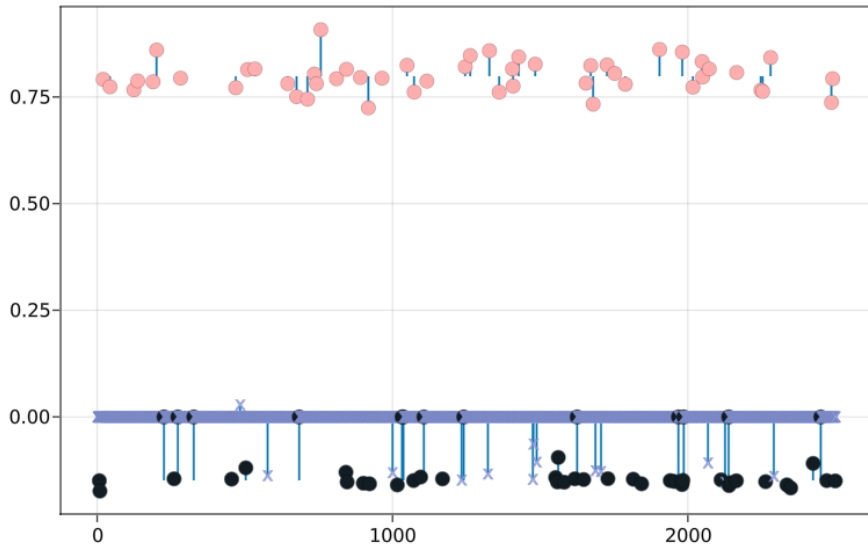


FIGURE 2: Posterior median estimate of x_k (where k can be identified with (i, j)) versus k computed using the Sticky Zig-Zag sampler. Thin vertical lines indicate distance to the truth. True zeros are plotted with the symbol \times , others are plotted as points. With $p = 50$ agents, the dimension of the problem is $d = 2450$

5.2 Spatially structured sparsity

We consider the problem of denoising a spatially correlated, sparse signal. The signal is assumed to be an $n \times n$ -image. Denote the observed pixel value at location (i, j) by $Y_{i,j}$ and assume

$$Y_{i,j} = x_{i,j} + Z_{i,j}, \quad Z_{i,j} \stackrel{\text{i.i.d.}}{\sim} \text{N}(0, \sigma^2), \quad i, j \in \{1, \dots, n\}.$$

The “true signal” is given by $x = \{x_{i,j}\}_{i,j}$ and this is the parameter we aim to infer, while assuming σ^2 to be known. We view x as a vector in \mathbb{R}^d , with $d = n^2$ but use both linear indexing x_k and Cartesian indexing $x_{i,j}$ to refer to the component at index $k = n(i - 1) + j$. The log-likelihood of the parameter x is given by $\ell(x) = C + \sigma^{-2} \sum_{i=1}^n \sum_{j=1}^n |x_{i,j} - Y_{i,j}|^2$, with C a constant not depending on x .

We consider the following prior measure

$$\mu_0(dx) = \exp\left(-\frac{1}{2}x'\Gamma x\right) \prod_{i=1}^d \left(dx_i + \frac{1}{\kappa}\delta_0(dx_i)\right).$$

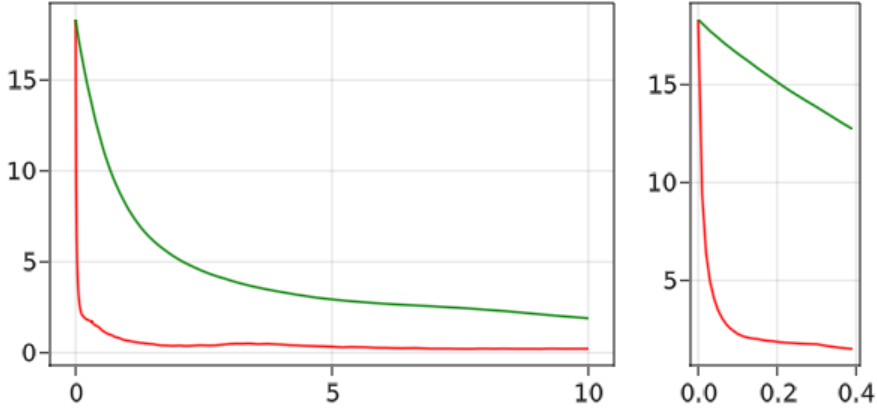


FIGURE 3: $c \rightarrow \mathcal{P}_{\text{zig-zag}}(c)$ (red) and $c \rightarrow \mathcal{P}_{\text{gibbs}}(c)$ (green) where c represent the computing time; right-panel: zoom-in near 0. With $p = 20$ agents the dimension of the problem is $p(p - 1)/2 = 380$.

The Dirac masses in the prior encapsulate sparseness in the underlying signal and an appropriate choice of Γ can promote smoothness. Overall, the prior encourages *smoothness, sparsity and local clustering of zero entries and non-zero entries*. As a concrete example, consider $\Gamma = c_1\Lambda + c_2I$ where Λ is the graph Laplacian of the pixel neighbourhood graph: the pixel indices i, j are identified with the vertices $V = \{(i, j) : (i, j) \in \{1, \dots, n\}^2\}$ of the $n \times n$ -lattice with edges $E = \{(v, v') : (v, v') = ((i, j), (i', j')) \in V^2, |i - i'| + |j - j'| = 1\}$ (using the set notation for edges). Thus, edges connect a pixel to its vertical and horizontal neighbours. Then

$$\lambda_{v,v'} = \begin{cases} \text{degree}(v) & v = v' \\ -1 & \{v, v'\} \in E \\ 0 & \text{otherwise} \end{cases}$$

and $\Lambda = (\Lambda_{k,l})_{k,l \in \{1, \dots, n^2\}}$ with $\Lambda_{(i-1)n+j, (k-1)n+l} = \lambda_{(i,j), (k,l)}$, for $i, j, k, l \in \{1, \dots, n\}$.

This is a prior which is applicable in similar situations as the fused Lasso in Tibshirani et al. (2005).

Numerical experiments: We assume that pixel (i, j) corresponds to a physical location of size $\Delta_1 \times \Delta_2$ centered at $u(i, j) = u_0 + (i\Delta_1, j\Delta_2) \in \mathbb{R}^2$. To numerically illustrate our approach, we use a heart shaped region given by $x_{i,j} = 5 \max(1 - h(u(i, j)), 0)$ where $h: \mathbb{R}^2 \rightarrow [0, \infty)$ is defined by $h(u_1, u_2) = u_1^2 + \left(\frac{5u_2}{4} - \sqrt{|u_1|}\right)^2$, $u_0 = (-4.5, -4.1)$, $n = 10^3$ and $\Delta_1 = \Delta_2 = 9/n$. In the example, about 97% of the pixels of the truth are black. The dimension of the parameter equals 10^6 . Figure 4, top-left, shows the observation Y with $\sigma^2 = 0.5$ and the ground truth.

As the ordinary Sticky Zig-Zag sampler would require storing and ordering 1 million elements in the priority queue we ran the Sticky Zig-Zag sampler with sparse implementation as detailed in Remark 3.1. For this example, we have $\Psi(x) = \ell(x) + 0.5x'\Gamma x$. We took $c_1 = 2, c_2 = 0.1$ in the definition of Γ and chose the parameters $\kappa_1 = \kappa_2 = \dots = \kappa_d = 0.15$ for the smoothing prior. The reflection times are computed by means of a thinning scheme, see Appendix D.3 for details. We set the final clock of the Sticky Zig-Zag sampler to 500. Results from running the sampler are summarized in Figure 4.

In Figure 5, the runtimes of the Sticky Zig-Zag sampler and Gibbs sampler are shown (in a log-log scale) for different values of n^2 (dimensionality of the problem), the final clock was fixed to $T = 500$ (10^3 iteration for the Gibbs sampler). All the other parameters are kept fixed as described above. The results agree well with the scaling results of Table 1, rightmost column.

In Figure 6 we show $t \rightarrow \mathcal{P}_{\text{Zig-Zag}}(t)$ and $t \rightarrow \mathcal{P}_{\text{Gibbs}}(t)$ for t ranging from 0 to 5, in case $n = 20$. Both samplers were initialized at the posterior mean of the Gaussian density proportional to Ψ (hence, in the full-model with no coordinates set to 0). In this experiment, the Sticky Zig-Zag sampler outperforms the Gibbs sampler considerably.

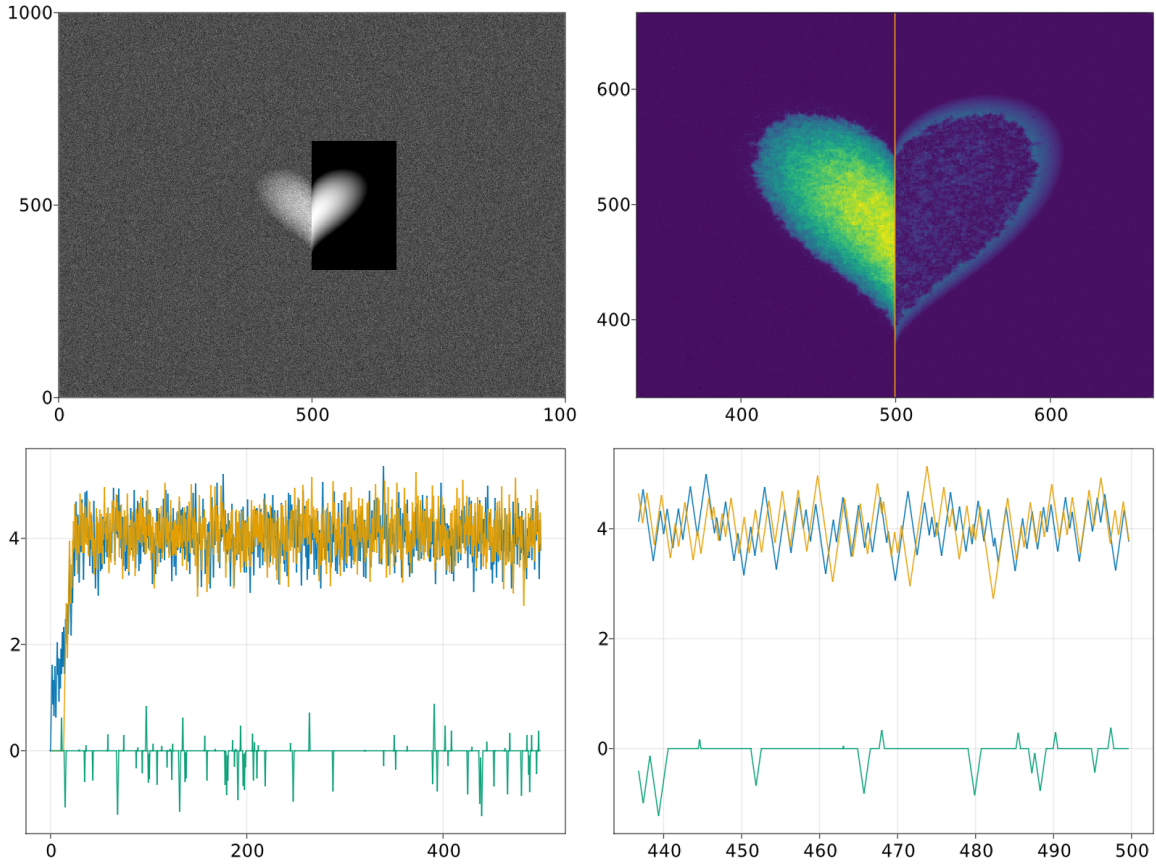


FIGURE 4: Top-left: observed 1000×1000 image of a heart corrupted with white noise, with part of the ground truth inset. Top-right, left half: posterior mean estimated from the trace of the Sticky Zig-Zag sampler (detail). Top-right, right half: mirror image showing the absolute error between the posterior mean and the ground truth in the same scale (color gradient between blue (0) and yellow (maximum error)). Bottom: trace plot of 3 coordinates; on the left the full trajectory is shown whereas on the right only the final 60 time units are displayed. The traces marked with blue and orange lines belong to neighbouring coordinates (highly correlated) from the center, the trace marked with green belongs to a coordinate outside the region of interest.

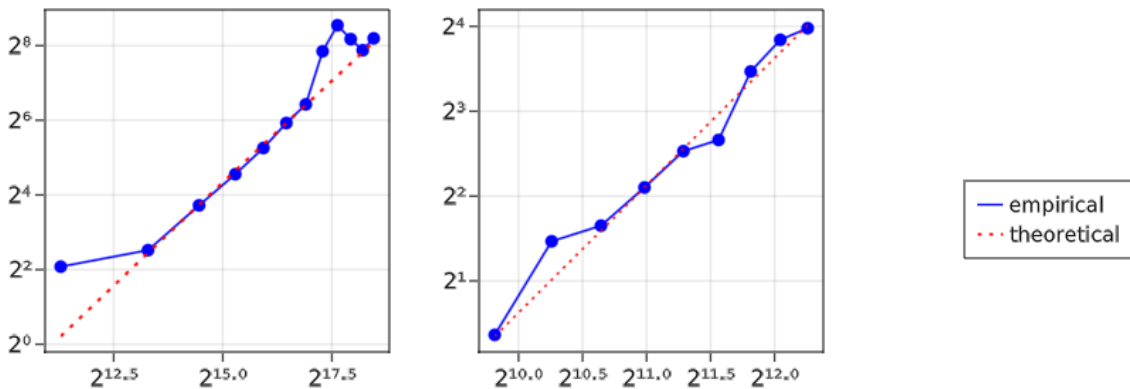


FIGURE 5: Blue: Runtime comparison of the Sticky Zig-Zag sampler (left) and the Gibbs sampler (right) for the example in Subsection 5.2. The horizontal axis displays the dimension of the problem, which is n^2 . The point on the left figure correspond to $n^2 = 50^2, 100^2, \dots, 600^2$; the point on the right figure to $n^2 = 40^2, 45^2, \dots, 70^2$. The vertical axis shows runtime in seconds. Both plots are on a log-log scale. Orange curves shows the theoretical scaling (including a log-factor for the priority queue insertion): $x \mapsto c_1 x \log(x)$ (left) and $x \mapsto c_2 x^{3/2}$ (right), with c_1 and c_2 chosen conveniently.

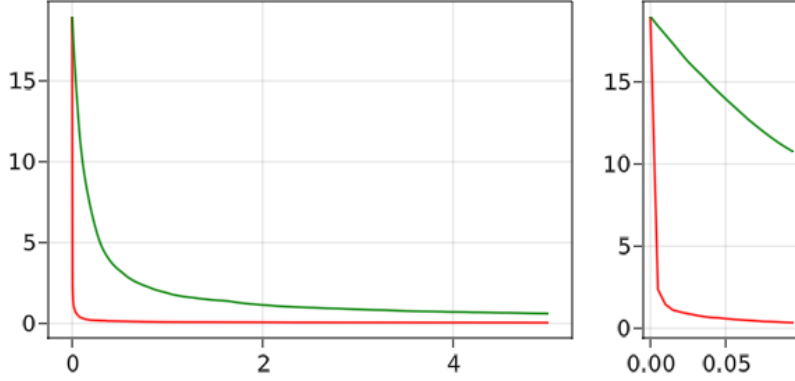


FIGURE 6: $c \rightarrow \mathcal{P}_{\text{zig-zag}}(c)$ (red) and $t \rightarrow \mathcal{P}_{\text{gibbs}}(c)$ (green) where c represent the computational power; right-panel: zoom-in near 0. Here the dimension of the problem is $n^2 = 400$.

5.3 Sampling from a strongly bimodal target

In this section we present an example where the Gibbs sampler has substantial difficulties exploring the state-space, while the Sticky Zig-Zag sampler performs well. Fix the functions $\mu^{(j)}: \mathbb{R} \rightarrow \mathbb{R}$ with $j = 1, 2, 3$ and grid points $t_0 < t_1 < \dots < t_n$. Let $x_{i,j} = \mu^{(j)}(t_i)$. Rather than considering the statistical model with observations $Y_{i,j} \sim \mathcal{N}(x_{i,j}, \sigma^2)$ (corresponding to a standard linear regression) we consider the model with observations $\bar{Y}_{i,j} \sim \mathcal{N}(x_{i,j} - x_{i-1,j}, \sigma^2)$, corresponding to observing increments of each $\mu^{(j)}$ with error. The likelihood of $\{\bar{Y}_{1,j}, \dots, \bar{Y}_{n,j}\}_{j=1,2,3}$ is given by (we omit dependence on the observations in the notation)

$$\ell(x) = C - \frac{1}{2\sigma^2} \sum_{j=1}^n \sum_{i=1}^n (x_{i,j} - x_{i-1,j} - \bar{Y}_{i,j})^2, \quad x = (x_0, x_1, \dots, x_n),$$

for some constant C which does not depend on x . As the likelihood is invariant under mapping each $x_{i,j}$ to $x_{i,j} + c_j$, it is clear that there is no unique maximum likelihood estimator. However, upon specification of a prior distribution, the posterior distribution is well defined. We impose a spike-and-slab prior on x (equation (1.1)), with each slab centered at zero and with variance σ_0^2 , thereby encouraging that flat parts of the curves $t \mapsto \mu^{(j)}(t)$ are located at the horizontal axis. Suppose the ground truth for $\mu := (\mu^{(1)}, \mu^{(2)}, \mu^{(3)})$ is given by

$$\mu^{(j)}(t_i) = c_j + \begin{cases} 0 & \text{if } j \neq 2 \\ 6t_i + 2\pi \cos(t_i) & \text{if } j = 2 \end{cases}, \quad t_i = 0, \frac{1}{n}2\pi, \dots, \frac{n-1}{n}2\pi, 2\pi.$$

for values $c_j \in \mathbb{R}$, $j = 1, 2, 3$. It is clear from the description that with this choice of μ and prior, the blocks of coordinates $\{x_{i,1}\}_{i=0,1,\dots,n}$ and $\{x_{i,3}\}_{i=0,1,\dots,n}$ are likely to be 0 and are mutually independent from the block $\{x_{i,2}\}_{i=0,1,\dots,n}$ and therefore acting as ‘background’ noise under the posterior (similarly to the black pixel in Section 5.2). The block $\{x_{i,2}\}_{i=0,1,\dots,n}$ will present bi-modality under the posterior as $t \rightarrow \mu^{(2)}(t)$ has 2 flat parts and the corresponding coefficients of each flat part are individually encouraged to concentrate a posteriori at the horizontal axis. Moreover, traversing from one mode to the other mode requires many parameters to be changed from zero to nonzero (and vice versa) simultaneously. The Gibbs sampler proposes a new (sub-)model uniformly at random, i.e., without using information from the data, and has difficulties to explore the posterior in this example. In contrast, this example shows that the Sticky Zig-Zag uses data information in exploring the models and tends to set those variables to zero which are small under the model currently explored (compare to the discussion in Section 4.3).

Numerical experiment: We set $n = 39$ and simulated data $\bar{Y}_{i,j}$ with $\sigma = 0$ (hence $\bar{Y}_{i,j} = \mu^{(j)}(t_i) - \mu^{(j)}(t_{i-1})$) for all $i = 1, 2, \dots, n$ and $j = 1, 2, 3$, whereas in the likelihood we took $\sigma = 0.6$. The

variance of the prior slabs are set to $\sigma_0^2 = 6.0$. The dimension of the problem is $3(n + 1) = 120$. Figure 7 shows the results for the Sticky Zig-Zag sampler (with $T = 5 \times 10^5$) and the Gibbs sampler (with 7×10^4 iterations) which have been simulated for a similar computing time with burn-in of the first 0.3 segment of the trajectory for the Sticky Zig-Zag (first 0.3 fraction of iterations for the Gibbs sampler). Both algorithms were initialized at $x(0) \sim \mathcal{N}_{3(n+1)}(0, I)$.

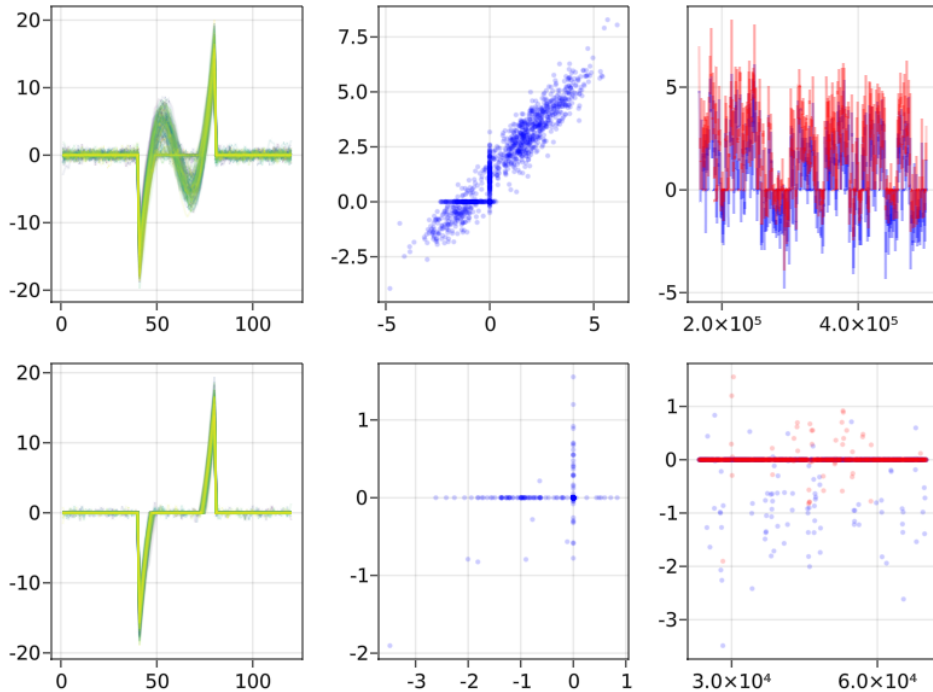


FIGURE 7: Visualization of the output of model with Gaussian increments. Top: Sticky Zig-Zag sampler. Bottom: Gibbs sampler. Left: trace of the vector ($\{x_{i,1}\}_{i=0,1,\dots,n}, \{x_{i,2}\}_{i=0,1,\dots,n}, \{x_{i,3}\}_{i=0,1,\dots,n}$) (the color gradient from yellow to blue indicates the sampling time). Center: (x_{48}, x_{49}) phase portrait (for clarity, we subsampled points of the Zig-Zag trajectories at every 250 unit times and sub-sampled points of the Gibbs sampler at every 70 iterations). Right: traces of x_{48} (blue) and x_{49} (red). Here, the dimension of the problem is $3(n + 1) = 120$. Here it is clear that, with the given computational budget, the Gibbs sampler fails to mix between different sub-models.

5.4 Logistic regression

Suppose $\{0, 1\} \ni Y_i \mid x \sim \text{Ber}(\psi(x^T a_i))$ with $\psi(u) = (1 + e^{-u})^{-1}$. $a_i \in \mathbb{R}^d$ denotes a vector of covariates and $x \in \mathbb{R}^d$ a parameter vector. Assume Y_1, \dots, Y_N are independent, conditional on x . The log-likelihood is equal to

$$\ell(x) = \sum_{j=1}^N \left(\log \left(1 + e^{\langle a_j, x \rangle} \right) - y_j \langle a_j, x \rangle \right)$$

We assume a spike-and-slab prior of (1.1) with zeromean Gaussian slabs and (large) variance σ_0^2 . Then the posterior can be written as in equation (1.2), with Ψ and κ as in equation (1.3).

Numerical experiments: We consider two categorical features with 30 levels each and 5 continuous features. For each observation, an independent random level of each discrete feature and a random value of the continuous features, $\mathcal{N}(0, 0.1^2)$ is drawn. Let the design matrix $A \in \mathbb{R}^{N \times d}$ be the matrix where the i -th row is the vector a_i . A includes the levels of the discrete features in dummy encoding and the interaction terms between them also in dummy encoding scaled by 0.3 (960 columns), and the continuous features in the final 5 columns. This implies that the dimension of the parameter equals

$d = 965$. We then generate $N = 50d = 48250$ observations using as ground truth sparse coefficients obtained by setting $x_i = z_i \xi_i$ where $z_i \stackrel{\text{i.i.d.}}{\sim} \text{Bern}(0.1)$ and $\xi_i \stackrel{\text{i.i.d.}}{\sim} \mathcal{N}(0, 5^2)$, where $\{z_i\}$ and $\{\xi_i\}$ are independent.

We run the sticky ZigZag with subsampling and bounding rates derived in Appendix D.2. We chose $w_1 = w_2 = \dots = w_d = 0.1$ and $\sigma_0^2 = 10^2$ and ran the Sticky Zig-Zag sampler for 100 time-units. The implementation makes use of a sparse matrix representation of A , speeding up the computation of inner products $\langle a_j, x \rangle$. Figure 8 reveals that while perfect recovery is not obtained (as was to be expected), most nonzero/zero features *are* recovered correctly.

In a second numerical experiment we compare the computing time of the Sticky Zig-Zag sampler and Gibbs sampler (as proposed in Polson, Scott, and Windle (2013)) as we vary the number of observations (N). In this case, we reduce the dimension of the parameter by restricting to 2 categorical variables, including their pairwise interactions, augmented by 3 “continuous” predictors (leading to the parameter vector $x \in \mathbb{R}^9$). For each sample size N we ran the Gibbs sampler for 1000 iterations and the Sticky Zig-Zag sampler for 1000 time units. Our interest here is not to compare the computing time of the samplers for a fixed value of N , but rather the scaling of each algorithm with N . Figure 9 shows that the computing time for the Sticky Zig-Zag sampler is roughly constant when varying N . On the contrary, the computing time increases linearly with N for the Gibbs sampler. This is consistent with the theoretical scaling results presented in Table 1 (rightmost column). We remark that qualitatively similar results would be obtained if we would have fixed the number of iterations of the Gibbs sampler and endtime of the Zig-Zag sampler to different values.

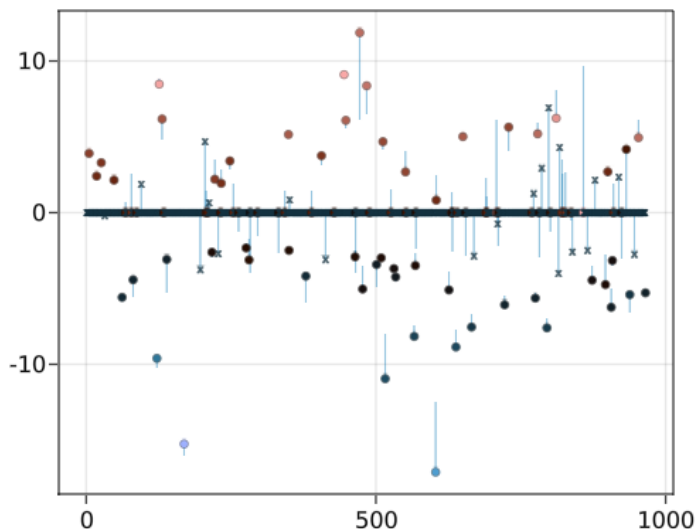


FIGURE 8: Results for the logistic regression coefficients derived with the Sticky Zig-Zag sampler with subsampling. Description as in caption of Figure 2. The dimension of this problem is $d = 965$.

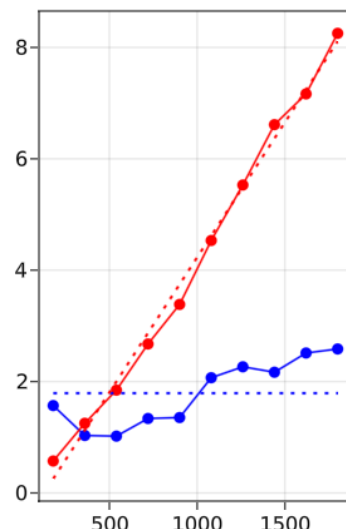


FIGURE 9: Logistic regression example: computing time in seconds versus number of observations. Solid red line: Gibbs samplers with 10^3 iterations. Solid blue line: Sticky Zig-Zag samplers with subsampling ran for 10^3 time units. The dashed lines correspond to the scaling results displayed in Table 1. Here, the dimension of the problem is fixed to $d = 9$.

5.5 Estimating a sparse precision matrix

Consider

$$Y_i | X \stackrel{\text{i.i.d.}}{\sim} \mathcal{N}_p(0, (XX')^{-1}), \quad i = 1, 2, \dots, N$$

for some unknown lower triangular sparse matrix $X \in \mathbb{R}^{p \times p}$. We aim to infer the lower-triangular elements of X which we concatenate to obtain the parameter vector $x := \{X_{i,j} : 1 \leq j \leq i \leq p\} \in \mathbb{R}^{d(d+1)/2}$. This class of problems is important as the precision matrix XX' unveils the conditional independence structure of Y , see for example Shi, Ghosal, and Martin (2021), and reference therein, for details.

We impose a prior measure on x of the product form $\mu_0(dx) = \bigotimes_{i=1}^p \bigotimes_{j=1}^i \mu_{i,j}(dx_{i,j})$ where

$$\mu_{i,j}(dx_{i,j}) = \begin{cases} \pi_{i,j}(x_{i,j}) \mathbf{1}_{(x_{i,j} > 0)} dx_{i,j} & i = j, \\ w\pi_{i,j}(x_{i,j}) dx_{i,j} + (1-w)\delta_0(dx_{i,j}) & i \neq j, \end{cases}$$

and $\pi_{i,j}$ is the univariate Gaussian density with mean $c_{i,j} \in \mathbb{R}$ and variance $\sigma_0^2 > 0$.

This prior induces sparsity on the lower-triangular off-diagonal elements of X while preserving strict positive definiteness of XX' (as the elements on the diagonal are restricted to be positive).

The posterior in this example is not of the form

$$\mu(dx) \propto \exp(-\Psi(x)) \left(\bigotimes_{i=1}^d \bigotimes_{j=1}^{i-1} (dx_{i,j} + \frac{1}{\kappa_{i,j}} \delta_0(dx_{i,j})) \right) \bigotimes_{k=1}^d dx_{k,k}$$

with

$$\Psi(x) = \frac{1}{2} \sum_{i=1}^N Y_i' X X' Y_i - N \sum_{i=1}^p \log(x_{i,i}) + \sum_{i=1}^p \sum_{j=1}^{i-1} \frac{(x_{i,j} - c_{i,j})^2}{2\sigma_0^2} + \sum_{i=1}^p \frac{(x_{i,i} - c_{i,i})^2}{2\sigma_0^2}$$

and $\kappa_{i,j} = \pi_{i,j}(0)w/(1-w)$. In particular, the posterior density is not of the form as given in equation (1.2), as the diagonal elements cannot be zero. Notice that, for any $i = 1, 2, \dots, p$, as $x_{i,i} \downarrow 0$, $\exp(-\Psi(x))$ vanishes and $\nabla \Psi(x) \rightarrow \infty$. This makes the sampling problem challenging for gradient-based algorithms.

Numerical experiments: We apply the Sticky Zig-Zag sampler where the reflection times are computed by using a thinning and superposition scheme for inhomogeneous Poisson processes, see Appendix D.4 for the details.

We simulate realisations y_1, \dots, y_N with precision matrix XX' a tri-diagonal matrix with diagonal $(0.5, 1, 1, \dots, 1, 1, 0.5) \in \mathbb{R}^p$ and off-diagonal $(-0.3, -0.3, \dots, -0.3) \in \mathbb{R}^{p-1}$. In the prior we chose $\sigma_0^2 = 10$ and $c_{i,j} = \mathbf{1}_{(i=j)}$ and for $1 \leq j \leq i \leq p$ and $w = 0.2$.

We fixed $N = 10^3$ and $p = 200$ and ran the Sticky Zig-Zag sampler for 600 time-units. We initialized the algorithm at $x(0) \sim \mathcal{N}_{p(p+1)/2}(0, I)$ and set a burn-in of 10 unit-time. Figure 10 left panel shows the error between XX' (the ground truth) and $\bar{X} \bar{X}'$ where \bar{X} is posterior mean of the lower triangular matrix estimated with the sampler. The error is concentrated on the non-zero elements of the matrix while the zero elements are estimated with essentially no error. Figure 10 right panel shows the trajectories of two representative non-zero elements of X . The traces show qualitatively that the process converges quickly to its stationary measure. In this case, comparisons with the Gibbs sampler are not possible as there is no closed form expression for the Bayes factors of equation (4.1).

6 Discussion

In what follows, we outline promising research directions deferred to future work.

6.1 Sticky Hamiltonian Monte Carlo

The ordinary Hamiltonian Monte Carlo (HMC) process as presented by Neal et al. (2011) can be seen as a piecewise deterministic Markov processes with deterministic dynamics equal to

$$\dot{x} = v, \quad \dot{v} = -\nabla \Psi(x) \tag{6.1}$$

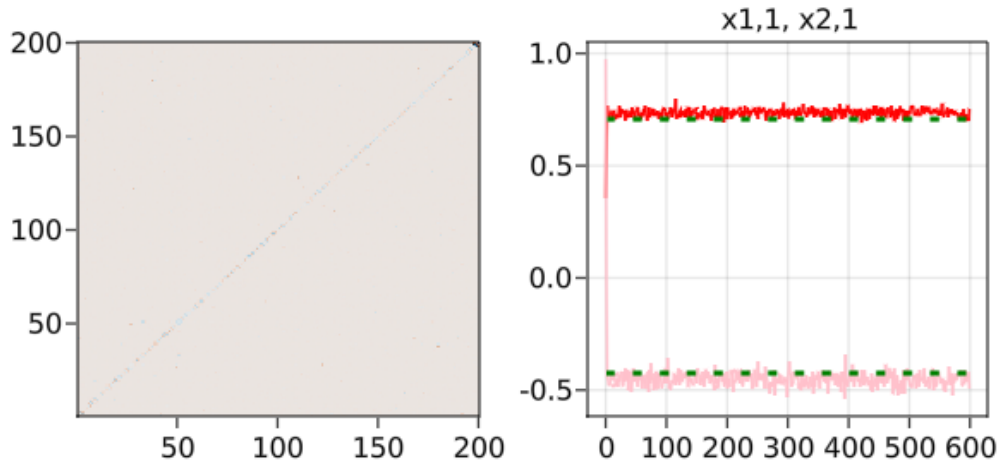


FIGURE 10: Left: error between the true precision matrix and the precision matrix obtained with the estimated posterior mean of the lower-triangular matrix (color gradient between white (no error) and black (maximum error)). Right: traces of two non-zero coefficients ($x_{1,1}$ in red and $x_{2,1}$ in pink) of the lower triangular matrix. Dashed green lines are the ground truth. Here, the dimension of each vector Y_i is $p = 200$ and the dimension of the problem is $p(p + 1)/2 = 20\,100$.

where $\nabla\Psi$ is the gradient of the negated log-density relative to the Lebesgue measure. At random exponential times with constant rate, the velocity component is refreshed as $v \sim \mathcal{N}(0, I)$ (similarly to the refreshment events in the bouncy particle sampler). By applying the same principles outlined in Section 2, such process can be made sticky with equation 1.2 as its stationary measure.

Unfortunately, in most cases, the dynamics in (6.1) cannot be integrated analytically so that a sophisticated numerical integrator is usually employed and a Metropolis-Hasting steps compensates for the bias of the numerical integrator (see Neal et al., 2011 for details). These two last steps makes the process effectively a discrete-time process and its generalization with sticky dynamics is not anymore trivial.

6.2 Extensions

The setting considered in this work does not incorporate some relevant classes of measures:

- Posteriors given by prior measures which freely choose prior weights for each (sub-)model. This limitation is mainly imputed to the parameter $\kappa = (\kappa_1, \kappa_2, \dots, \kappa_d)$ which here does not depend on the location component x of the state space. While the theoretical framework built can be easily adapted for letting κ depend on x , it is currently unclear to us the exact relationship between κ and the posterior measure in this more general setting.
- measures which are not supported on neighbouring sub-models are also not covered here. For example, consider the space \mathbb{R}^2 and assumes that the process can visit either the origin $(0, 0)$ or the full space \mathbb{R}^2 but not the coordinate axes $\{0\} \times \mathbb{R} \cup \mathbb{R} \times \{0\}$. Then the process started in \mathbb{R}^2 hits the origin with probability 0, hence failing to explore the subspace $(0, 0)$. To solve this problem, different dynamics for the process should be developed.

Acknowledgement: this work is part of the research programme *Bayesian inference for high dimensional processes* with project number 613.009.034c, which is (partly) financed by the Dutch Research Council (NWO) under the *Stochastics – Theoretical and Applied Research* (STAR) grant. J. Bierkens acknowledges support by the NWO for the research project *Zig-zagging through computational barriers* with project number 016.Vidi.189.043.

References

- [1] C. Andrieu and S. Livingstone. “Peskun-Tierney ordering for Markov chain and process Monte Carlo: beyond the reversible scenario”. In: (2019). arXiv: 1906.06197.
- [2] J. Bento, M. Ibrahimi, and A. Montanari. “Learning Networks of Stochastic Differential Equations”. In: (2010). arXiv: 1011.0415.
- [3] J. Bierkens, P. Fearnhead, and G. Roberts. “The Zig-Zag process and super-efficient sampling for Bayesian analysis of big data”. In: *Ann. Statist.* 47.3 (June 2019), pp. 1288–1320.
- [4] J. Bierkens, S. Grazzi, K. Kamatani, and G. Roberts. “The boomerang sampler”. In: *International conference on machine learning*. PMLR. 2020, pp. 908–918.
- [5] J. Bierkens, S. Grazzi, F. van der Meulen, and M. Schauer. “A piecewise deterministic Monte Carlo method for diffusion bridges”. In: *Statistics and Computing* 31.3 (2021), pp. 1–21.
- [6] A. Bouchard-Côté, S. J. Vollmer, and A. Doucet. “The Bouncy Particle Sampler: A Non-Reversible Rejection-Free Markov Chain Monte Carlo Method”. In: *Journal of the American Statistical Association* 113.522 (2018), pp. 855–867.
- [7] A. Chevallier, P. Fearnhead, and M. Sutton. *Reversible Jump PDMP Samplers for Variable Selection*. 2020. arXiv: 2010.11771.
- [8] H. Chipman et al. “The practical implementation of Bayesian model selection”. In: *Lecture Notes-Monograph Series* (2001), pp. 65–134.
- [9] S. L. Cotter, G. O. Roberts, A. M. Stuart, and D. White. “MCMC methods for functions: modifying old algorithms to make them faster”. In: *Statistical Science* (2013), pp. 424–446.
- [10] M. H. A. Davis. *Markov models and optimization*. Vol. 49. Monographs on Statistics and Applied Probability. Chapman & Hall, London, 1993.
- [11] S. Duane, A. D. Kennedy, B. J. Pendleton, and D. Roweth. “Hybrid Monte Carlo”. In: *Physics letters B* 195.2 (1987), pp. 216–222.
- [12] E. I. George and R. E. McCulloch. “Variable selection via Gibbs sampling”. In: *Journal of the American Statistical Association* 88.423 (1993), pp. 881–889.
- [13] S. Grazzi and M. Schauer. *Boid animation*. <https://youtu.be/01VoURPwVLI>. Youtube, 2021. URL: <https://youtu.be/01VoURPwVLI>.
- [14] P. J. Green. “Reversible jump Markov chain Monte Carlo computation and Bayesian model determination”. In: *Biometrika* (1995), p. 16.
- [15] P. J. Green and D. I. Hastie. “Reversible jump MCMC”. In: *Genetics* 155.3 (2009), pp. 1391–1403.
- [16] J. E. Griffin and P. J. Brown. “Bayesian global-local shrinkage methods for regularisation in the high dimension linear model”. In: *Chemometrics and Intelligent Laboratory Systems* (2021), p. 104255.
- [17] Y. Guan and M. Stephens. “Bayesian variable selection regression for genome-wide association studies and other large-scale problems”. In: *The Annals of Applied Statistics* 5.3 (2011), pp. 1780–1815.
- [18] H. Ishwaran and J. S. Rao. “Spike and slab variable selection: Frequentist and Bayesian strategies”. In: *The Annals of Statistics* 33.2 (2005), 730–773. ISSN: 0090-5364.
- [19] JuliaCon 2020 by Jesse Bettencourt. “*JuliaCon 2020 — Boids: Dancing with Friends and Enemies*”. 2020. URL: <https://www.youtube.com/watch?v=8gS6wejsGsY>.
- [20] X. Liang, S. Livingstone, and J. Griffin. “Adaptive random neighbourhood informed Markov chain Monte Carlo for high-dimensional Bayesian variable Selection”. In: *arXiv preprint arXiv:2110.11747* (2021).

- [21] T. M. Liggett. *Continuous time Markov processes*. Vol. 113. Graduate Studies in Mathematics. American Mathematical Society, Providence, RI, 2010.
- [22] T. J. Mitchell and J. J. Beauchamp. “Bayesian variable selection in linear regression”. In: *Journal of the American Statistical Association* 83.404 (1988), pp. 1023–1032.
- [23] R. M. Neal et al. “MCMC using Hamiltonian dynamics”. In: *Handbook of markov chain monte carlo* 2.11 (2011), p. 2.
- [24] N. G. Polson, J. G. Scott, and J. Windle. “Bayesian inference for logistic models using Pólya–Gamma latent variables”. In: *Journal of the American statistical Association* 108.504 (2013), pp. 1339–1349.
- [25] K. Ray, B. Szabo, and G. Clara. “Spike and slab variational Bayes for high dimensional logistic regression”. In: (2020). arXiv: 2010.11665.
- [26] C. W. Reynolds. “Flocks, Herds and Schools: A Distributed Behavioral Model”. In: Association for Computing Machinery, 1987.
- [27] L. C. G. Rogers and D. Williams. *Diffusions, Markov processes and martingales: Volume 2, Itô calculus*. Vol. 2. Cambridge university press, 2000.
- [28] L. Rogers and D. Williams. *Diffusions, Markov Processes, and Martingales: Volume 1, Foundations*. Cambridge Mathematical Library. Cambridge University Press, 2000.
- [29] M. Schauer and S. Grazi. *mschauer/ZigZagBoomerang.jl: v0.6.0*. Version v0.6.0. Mar. 2021. URL: <https://doi.org/10.5281/zenodo.4601534>.
- [30] W. Shi, S. Ghosal, and R. Martin. “Bayesian estimation of sparse precision matrices in the presence of Gaussian measurement error”. In: *Electronic Journal of Statistics* 15.2 (2021), pp. 4545–4579.
- [31] M. Sutton and P. Fearnhead. “Concave-Convex PDMP-based sampling”. In: *arXiv preprint arXiv:2112.12897* (2021).
- [32] R. Tibshirani et al. “Sparsity and smoothness via the fused lasso”. In: *Journal of the Royal Statistical Society: Series B (Statistical Methodology)* 67.1 (2005), pp. 91–108.
- [33] G. Zanella and G. Roberts. “Scalable importance tempering and Bayesian variable selection”. In: *Journal of the Royal Statistical Society: Series B (Statistical Methodology)* 81.3 (2019), pp. 489–517.

A Details of the Sticky Zig-Zag sampler

A.1 Construction

In this section we discuss how the Sticky Zig-Zag can be constructed as a *standard* PDMP in the sense of Davis (1993). The construction is a bit tedious, but the underlying idea is simple: the Sticky Zig-Zag process has the dynamics of an ordinary Zig-Zag process until it reaches a freezing boundary $\mathfrak{F}_i = \{(x, v) \in E: x_i = 0^-, v_i > 0 \text{ or } x_i = 0^+, v_i < 0\}$ of $E = \overline{\mathbb{R}}^d \times \mathcal{V}$, with $\overline{\mathbb{R}} = (-\infty, 0^-] \sqcup [0^+, \infty)$ which has two copies of 0. Then it immediately changes dynamics and evolves as a lower dimensional ordinary Zig-Zag process *on the boundary*, at least until an unfreezing event happens or upon reaching yet another freezing boundary in the domain of the restricted process.

Davis' construction allows a standard PDMP to make instantaneous jumps at boundaries of open sets, but puts restrictions on further behaviour at that boundary. We circumvent these restrictions by first splitting up the space $\mathbb{R}^d \times \mathcal{V}$ into disconnected components in a way somewhat different than the construction of E as presented in Section 2. Only at a later stage we recover the definition of E .

Define the set

$$K = \{\rightarrow\circ, \circ\rightarrow, \leftarrow\circ, \circ\leftarrow, \overset{\leftarrow}{\circ}, \overset{\rightarrow}{\circ}\}$$

and

$$|K| = \{\circ, \leftarrow\circ\rightarrow, \rightarrow\circ\leftarrow\}$$

(note that $|K|$ does not denote the cardinality of the set K). Define the functions $k: \mathbb{R} \times \mathbb{R} \rightarrow K$ and $|k|: \mathbb{R} \times \mathbb{R} \rightarrow |K|$ by

(x, v)	$k(x, v)$	at (x, v) the process is...	$ k (x, v)$
$x > 0, v > 0$	$\circ\rightarrow$...moving away from 0 with positive velocity	$\leftarrow\circ\rightarrow$
$x < 0, v < 0$	$\leftarrow\circ$...moving away from 0 with negative velocity	$\leftarrow\circ\rightarrow$
$x > 0, v < 0$	$\circ\leftarrow$...moving toward 0 with negative velocity	$\rightarrow\circ\leftarrow$
$x < 0, v > 0$	$\rightarrow\circ$...moving toward 0 with positive velocity	$\rightarrow\circ\leftarrow$
$x = 0, v > 0$	$\overset{\rightarrow}{\circ}$...at 0 with positive velocity	\circ
$x = 0, v < 0$	$\overset{\leftarrow}{\circ}$...at 0 with negative velocity	\circ

If $(x, v) \in \mathbb{R}^d \times \mathcal{V}$, then extend $k: \overline{\mathbb{R}}^d \times \mathcal{V} \rightarrow K^d$ and $|k|: \overline{\mathbb{R}}^d \times \mathcal{V} \rightarrow |K|^d$ by applying the map k and $|k|$ coordinatewise.

For each $\ell \in K^d$ define

$$\tilde{E}_\ell^\circ = \{(\ell, x, v): k(x, v) = \ell\}$$

Note that for $\ell \neq \ell'$ the sets \tilde{E}_ℓ° and $\tilde{E}_{\ell'}^\circ$ are disjoint. The set \tilde{E}_ℓ° is open under the metric introduced in Davis (1993), p.58, which sets the distance between two points (ℓ, x, v) and (ℓ', x', v') to 1 if $\ell \neq \ell'$. We denote the induced topology on \tilde{E} by $\tilde{\tau}$. \tilde{E}_ℓ° is a subset of \mathbb{R}^{2d} of dimension $d_\ell = \sum_{i=1}^d \mathbb{1}_{|\ell_i| \neq \circ}$, since the velocities are constant in \tilde{E}_ℓ° and the position of the components i where $\ell_i = \circ$ are constant as well in \tilde{E}_ℓ° (\tilde{E}_ℓ° is isomorphic to an open subset of \mathbb{R}^{d_ℓ}).

The sets which contain a singleton, i.e. $|\tilde{E}_\ell^\circ| = 1$, are those sets \tilde{E}_ℓ° such that $|\ell_i(x, v)| = \circ$ for all $i = 1, 2, \dots, d$ and are open as they contain one isolated point, but will have to be treated a bit differently. Then $\tilde{E}^\circ = \bigcup_{\ell \in K^d} \tilde{E}_\ell^\circ$ is the tagged space of open subsets of \mathbb{R}^{d_ℓ} used in Davis (1993, Section 24).

\tilde{E}° separates the space into isolated components of varying dimension. In each component, the Sticky Zig-Zag process behaves differently and essentially as a lower dimensional Zig-Zag process.

Let $\partial\tilde{E}_\ell^\circ$ denote the boundary of \tilde{E}_ℓ° in the embedding space \mathbb{R}^{d_ℓ} (where the velocity components are constant in \tilde{E}_ℓ°), with elements written (ℓ, x, v) . Some points in $\partial\tilde{E}_\ell^\circ$ will also belong to the state space \tilde{E} of the Sticky Zig-Zag process, but only the entrance-non-exit boundary points:

$$\tilde{E} = \bigcup_{\ell} \tilde{E}_\ell, \quad \tilde{E}_\ell = \tilde{E}_\ell^\circ \cup \{(\ell, x, v) \in \partial\tilde{E}_\ell^\circ : x_i = 0 \Rightarrow |\ell_i| \neq \rightarrow \circ \leftarrow \text{ for all } i\}.$$

(This corresponds to the definition of the state space in Davis (1993, Section 24), only that we use knowledge of the flow.)

The remaining part of the boundary is

$$\Gamma = \bigcup_{\ell} \Gamma_\ell \subset \bigcup_{\ell} \partial\tilde{E}_\ell^\circ, \quad \Gamma_\ell = \{(\ell, x, v) \in \partial\tilde{E}_\ell^\circ, \exists i: x_i = 0, |\ell_i| = \rightarrow \circ \leftarrow\},$$

with $\tilde{E} \cap \Gamma = \emptyset$ so that Γ is not part of the state space \tilde{E} . Any trajectory approaching Γ , jumps back into \tilde{E} just before hitting Γ . If \tilde{E}_ℓ° is a singleton ($|\tilde{E}_\ell^\circ| = 1$), then $\Gamma_\ell = \emptyset$ and $\tilde{E}_\ell = \tilde{E}_\ell^\circ$ (atoms).

Lemma A.1. *A bijection $\iota: \tilde{E} \rightarrow E$ is given by*

$$\iota((\ell, \tilde{x}, v)) = (x, v)$$

where

$$x_i = \begin{cases} 0^+ (0^-) & \ell_i = \bar{\circ} \ (\ell_i = \bar{\circ}) \\ 0^+ (0^-) & \ell_i = \circ \rightarrow \ (\ell_i = \leftarrow \circ), \tilde{x}_i = 0 \\ \tilde{x}_i & \text{otherwise.} \end{cases}$$

Proof. Recall that $\alpha(x, v) := \{i \in \{1, 2, \dots, d\} : (x, v) \notin \mathfrak{F}_i\}$ and α^c denotes its complement. First of all, notice that $\iota(\tilde{E}) \subset E$. Now let $(x, v) \in E$ be given. We construct $e \in \tilde{E}$ such that $(x, v) = \iota(e)$. If there is at least one $x_j = 0^\pm$ with $j \notin \alpha(x, v)$, then take $e = (\ell, \tilde{x}, v) \in \tilde{E} \setminus \tilde{E}^\circ$ as follows (entrance-non-exit boundary): for $i \in \alpha^c$ we have $|\ell_i| = \circ$, $\tilde{x}_i = 0$, while for all $i \in \alpha$ with $x_i = 0^\pm$, we have $|\ell_i| = \leftarrow \circ \rightarrow$, $\tilde{x}_i = 0$. Then $\iota(e) = (x, v)$. Otherwise, $e = (k(\tilde{x}, v), \tilde{x}, v) \in \tilde{E}^\circ$ (interior of an open set) and $\iota(e) = (x, v)$ where $\tilde{x}_i = 0$ for all $i \in \alpha(x, v)$ and $\tilde{x}_i = x_i$ otherwise. □

Having constructed the state space, we proceed with the process dynamics. Firstly, the deterministic flow (locally Lipschitz for every $\ell \in K$) is determined by the functions $\tilde{\phi}_\ell: [0, \infty) \times \tilde{E}_\ell^\circ \rightarrow \tilde{E}_\ell^\circ$ which for the sticky ZigZag process are given by

$$\tilde{\phi}(t, \ell, x, v) = (\ell, x', v), \quad \forall (\ell, x, v) \in \tilde{E},$$

with $x_i + v_i t (\mathbb{1}_{|\ell_i| \neq \circ})$, $i = 1, 2, \dots, d$ and determines the vector fields

$$\mathfrak{X}_\ell \tilde{f}(\ell, x, v) = \sum_{i=1}^d \mathbb{1}_{|\ell_i| \neq \circ} v_i \partial_{x_i} f(\ell, x, v), \quad f \in C^1(\tilde{E}).$$

Sometimes we write $\tilde{\phi}_k(t, x, v) = \tilde{\phi}(t, k, x, v)$ for convenience. Next, further state changes of the process are instantaneous, deterministic jumps from the boundary Γ into \tilde{E}

$$\mathcal{Q}^f((\ell, x, v), \cdot) = \delta_{(k(x, v), x, v)}, \quad (\ell, x, v) \in \Gamma$$

and random jumps at random times corresponding to unfreezing events

$$\mathcal{Q}^s((\ell, x, v), \cdot) = \frac{\sum_i \lambda_i^s(\ell, x, v) \delta_{(\ell[i: \ell'_i], x, v)}}{\sum_i \lambda_i^s(i, x, v)}$$

with $\ell'_i = \circ \rightarrow$ if $\ell_i = \vec{\circ}$ and $\ell'_i = \circ \leftarrow$ if $\ell_i = \overleftarrow{\circ}$, and random reflections

$$\mathcal{Q}^r((\ell, x, v), \cdot) = \frac{\sum_i \lambda_i^r(\ell, x, v) \delta_x \delta_{v[i: -v_i]} \delta_\ell}{\sum_i \lambda_i^r(\ell, x, v)}$$

with

$$\lambda_i^s(\ell, x, v) = \mathbb{1}_{|\ell_i|=\circ} \kappa_i$$

and

$$\lambda_i^r(\ell, x, v) = \mathbb{1}_{\ell_i \neq \circ} \left((v_i \partial_i \Psi(x))^+ + \lambda_{0,i}(x) \right), \quad i = 1, 2, \dots, d.$$

Then $\lambda: \tilde{E} \rightarrow \mathbb{R}^+$

$$\lambda(\ell, x, v) = \sum_{i=1}^d \lambda_i^r(\ell, x, v) + \lambda_i^s(i, x, v)$$

and a Markov kernel $\mathcal{Q}: (\tilde{E} \cup \Gamma, \mathcal{B}(\tilde{E} \cup \Gamma)) \rightarrow [0, 1]$ by

$$\mathcal{Q}((\ell, x, v), \cdot) = \begin{cases} \frac{\sum_i \lambda_i^r(\ell, x, v)}{\lambda(\ell, x, v)} \mathcal{Q}^r((\ell, x, v), \cdot) + \frac{\sum_i \lambda_i^s(\ell, x, v)}{\lambda(\ell, x, v)} \mathcal{Q}^s((\ell, x, v), \cdot) & (\ell, x, v) \in \tilde{E}, \\ \mathcal{Q}^f((\ell, x, v), \cdot) & (\ell, x, v) \in \Gamma. \end{cases}$$

Proposition A.2. $\mathfrak{X}, \lambda, \mathcal{Q}$ satisfy the standard conditions given in Davis (1993, Section 24.8), namely

- For each $\ell \in K$, \mathfrak{X}_ℓ is a locally Lipschitz continuous vector field and determines the deterministic flow $\tilde{\phi}_\ell: \tilde{E}_\ell \rightarrow \tilde{E}_\ell$ of the PDMP.
- $\lambda: \tilde{E} \rightarrow \mathbb{R}^+$ is measurable and such that $t \rightarrow \lambda(\tilde{\phi}_\ell(t, x, v))$ is integrable on $[0, \varepsilon(\ell, x, v))$, for some $\varepsilon > 0$, for each ℓ, x, v .
- $\mathcal{Q}: \tilde{E} \cup \Gamma \rightarrow \mathcal{P}(\tilde{E})$ is measurable and such that $\mathcal{Q}(\{(\ell, x, v)\}, (\ell, x, v)) = 0$
- The expected number of events up to time t , starting at (ℓ, x, v) is finite for each $t > 0, \forall (\ell, x, v) \in \tilde{E}$

To see the latter, remember that for any initial point $(\ell, x, v) \in \tilde{E}$, the deterministic flow (without any random event) hits Γ at most d times before reaching the singleton $(0, 0, \dots, 0)$ and being constant there.

A.2 Strong Markov property

Proposition A.3. (Part of Theorem 2.3) Let (\tilde{Z}_t) be a Zig-Zag process on \tilde{E} with characteristics $\mathfrak{X}, \lambda, \mathcal{Q}$. Then $Z_t = \iota(\tilde{Z}_t)$ is a strong Markov process.

Proof. By Davis (1993), Theorem 26.14, the domain of the extended generator of the process (\tilde{Z}_t) with characteristics $\mathfrak{X}, \lambda, \mathcal{Q}$ is

$$\mathcal{D}(\tilde{\mathcal{A}}) = \{f \in \mathcal{M}(\tilde{E}); t \rightarrow f(\tilde{\phi}_\ell(t, x, v)) \text{ } \tilde{\tau}\text{-absolutely continuous } \forall (\ell, x, v) \in \tilde{E}, t = [0, t_\Gamma(\ell, x, v)); \\ f(\ell, x, v) = f(\kappa(x, v), x, v), \quad (\ell, x, v) \in \Gamma\},$$

with

$$t_\Gamma(\ell, x, v) = \inf\{0 \leq t: \tilde{\phi}_\ell(t, x, v) \in \tilde{\Gamma}\}$$

and

$$\tilde{\mathcal{A}}f(\ell, x, v) = \mathfrak{X}_\ell f(\ell, x, v) + \lambda(\ell, x, v) \int_{\tilde{E}} (f(\ell', x', v') - f(\ell, x, v)) \mathcal{Q}(\ell, x, v, d(\ell', x', v')).$$

The strong Markov property of (\tilde{Z}_t) follows by Davis (1993), Theorem 25.5. Denote by $(\tilde{P}_t)_{t \geq 0}$ the Markov transition semigroup of (\tilde{Z}_t) and let $(P_t)_{t \geq 0}$ be a family of probability kernels on E and such that for any bounded measurable function $f: E \rightarrow \mathbb{R}$ and any $t \geq 0$,

$$\tilde{P}_t(f \circ \iota) = (P_t f) \circ \iota.$$

Then $(P_t)_{t \geq 0}$ is the Markov transition semigroup of the process $Z_t = (\iota(\tilde{Z}_t))$. By Rogers and Williams (2000b), Lemma 14.1, and since any stopping time for the filtration of (\tilde{Z}_t) is a stopping time for the filtration of (Z_t) , Z_t is a *strong* Markov process. □

A.3 Feller property

Given an initial point $\ell, x, v \in \tilde{E}$, let

$$t_{\Gamma_1}(\ell, x, v) = \inf\{0 \leq t: \tilde{\phi}_\ell(t, x, v) \in \tilde{\Gamma}\}$$

and define the *extended deterministic flow* $\tilde{\varphi}: \tilde{E} \rightarrow \tilde{E}$ by setting $\varphi(0, \ell, x, v) = (\ell, x, v)$ and recursively by

$$\tilde{\varphi}(t, \ell, x, v) = \begin{cases} \tilde{\varphi}_\ell(t, x, v) & t < t_{\Gamma_1}, \\ \tilde{\varphi}(t - t_{\Gamma_1}, k(x', v'), x', v') & t \geq t_{\Gamma_1} \end{cases}$$

with $(\ell', x', v') = \lim_{t \rightarrow t_{\Gamma_1}} \tilde{\varphi}_\ell(t, x, v) \in \Gamma$.

Observe that $t \rightarrow \iota(\tilde{\varphi}(t, \ell, x, v))$ is continuous on (E, τ) . Define also

$$\Lambda(t, \ell, x, v) = \int_0^t \lambda(\tilde{\varphi}(s, \ell, x, v)) ds.$$

Notice that, while $(\ell, x, v) \rightarrow \lambda(\ell, x, v)$ has discontinuities at the boundaries Γ , $(\ell, x, v) \rightarrow \Lambda(\ell, x, v)$ is continuous. Denote by T_1 the first random event (so excluding the deterministic jumps). Then for functions $f \in B(\tilde{E})$ and $\psi \in B(\mathbb{R}^+ \times \tilde{E})$, set $z(t) = (\ell(t), x(t), v(t))$ and define

$$\tilde{G}\psi(t, \ell, x, v) = E[f(z(t)) \mathbb{1}_{t < T_1} + \psi(t - T_1, z(t)) \mathbb{1}_{t \geq T_1}].$$

We have that

$$\tilde{G}\psi(t, \ell, x, v) = f(\tilde{\varphi}(t, \ell, x, v)) \times \mathcal{T} \tag{A.1}$$

with

$$\mathcal{T} = \sum_i \int_0^t \mathbf{1}_{t \in [t_i^\Gamma, t_{i+1}^\Gamma)} \int_{x', v'} \psi(t - s, \ell, x, v) \mathcal{Q}((\ell, dx', dv'), \tilde{\varphi}(s, \ell, x, v)) \lambda(\tilde{\varphi}(s, \ell, x, v)) e^{-\Lambda(s, \ell, x, v)} ds.$$

The Feller property holds if, for each fixed t and for $f \in C_b(E)$, we have that $(x, v) \rightarrow P_t f(x, v)$ is continuous (and bounded follows easily). This is what we are going to prove below, by making a detour in the space \tilde{E} , using the bijection ι and adapting some results found in Davis (1993, Section 27), for the process \tilde{Z}_t .

Theorem A.4. (Part of Theorem 2.3) Z_t is a Feller process.

Proof. Take $f \in C_b(\tilde{E})$ such that $f \circ \iota \in C_b(E)$. Call those functions on \tilde{E} τ -continuous. We want to show that \tilde{P} preserves τ -continuity. Notice that τ -continuous functions on \tilde{E} are such that

$$\lim_{t \rightarrow t_\Gamma} f(\tilde{\varphi}(t, \ell, x, v)) = f(\tilde{\varphi}(t_\Gamma, \ell, x, v)), \quad (\ell, x, v) \in \tilde{E}.$$

For τ -continuous functions f and for a fixed t , the first term on the right hand side of (A.1) $(\ell, x, v) \rightarrow f(\tilde{\varphi}(t, \ell, x, v))$ is clearly continuous. Also the second term is continuous since is of the form of an

integral of a piecewise continuous function. Therefore, for any $t \geq 0$, $\psi(t, \cdot) \in B(\tilde{E})$ and τ -continuous function f , we have that $(\ell, x, v) \rightarrow \tilde{G}\psi(t, \ell, x, v)$ is continuous. Clearly, the (similar) operator

$$\tilde{G}_n\psi_\ell(t, x, v) = E_x[f(\tilde{\varphi}_\ell(t, x, v))\mathbb{1}_{t < T_n} + \psi(t - T_n, \tilde{\varphi}_\ell(t, x, v))\mathbb{1}_{t \geq T_n}],$$

with T_n denoting the n th random time, is continuous as well for any fixed n, t , $\psi(t, \cdot) \in B(\tilde{E})$ and τ -continuous function f . By applying Lemma 27.3 in Davis (1993) we have that for any $\psi(t, \cdot) \in B(\tilde{E})$

$$|\tilde{G}_n\psi_\ell(t, x, v) - \tilde{P}_t f(x, v)| \leq 2 \max(\|\psi\| \|f\|) P(t \geq T_n).$$

Finally, if λ is bounded, then we can bound $P(t \geq T_n)$ by something which does not depend on (ℓ, x, v) and goes to 0 as $n \rightarrow \infty$ so that $\tilde{G}_n\psi \rightarrow \tilde{P}_t f$ uniformly on $\ell, x, v \in \tilde{E}$ under the supremum norm. This shows that, for any t , \tilde{P}_t (and therefore P_t) preserves τ -continuity. \square

Remark A.5. The proof of the Feller and Markov property follow similarly for the Bouncy Particle and the Boomerang sampler.

A.4 The extended generator of Z_t

Let $f \in \mathcal{D}(\mathcal{A})$ if $\tilde{f} \in \mathcal{D}(\tilde{\mathcal{A}})$ and $f \circ \iota = \tilde{f}$. Then $f \in \mathcal{D}(\mathcal{A})$ are τ -absolutely continuous functions along full deterministic trajectories on E :

$$\begin{aligned} \mathcal{D}(\mathcal{A}) = \{f \in \mathcal{M}(E); t \rightarrow f(\varphi(t, x, v)) \text{ } \tau\text{-absolutely continuous } \forall (x, v); \\ \lim_{t \rightarrow 0} f(x[i: 0^+ + t], v) = f(x[i: 0^+], v); \\ \lim_{t \rightarrow 0} f(x[i: 0^- - t], v) = f(x[i: 0^-], v)\}. \end{aligned}$$

For those functions $f \in \mathcal{D}(\mathcal{A})$ with $f \circ \iota = \tilde{f}$ we have that

$$\tilde{\mathcal{A}}\tilde{f}(\ell, \tilde{x}, v) = \mathcal{A}f(x, v) = \sum_{i=1}^N \mathcal{A}_i f(x, v)$$

with

$$\mathcal{A}_i f(x, v) = \begin{cases} \kappa_i(f(T_i(x, v)) - f(x, v)) & (x, v) \in \mathfrak{F}_i, \\ v_i \partial_{x_i} f(x, v) + \lambda_i(x, v)(f(x, v[i: -v_i]) - f(x, v)), & \text{otherwise,} \end{cases}$$

and

$$\lambda_i(x, v) = (v_i \partial_i \Psi(x))^+ + \lambda_{0,i}(x), \quad i = 1, 2, \dots, d,$$

for positive functions $\lambda_{0,i}$.

Proposition A.6. (Proposition 2.1) The extended generator of the process $(Z(t))$ is given by \mathcal{A} with domain $\mathcal{D}(\mathcal{A})$.

Proof. This is to verify that if $f \in \mathcal{D}(\tilde{\mathcal{A}})$ and $\tilde{\mathcal{A}}$ solve the martingale problem, i.e are such that

$$f(\ell(t), x(t), v(t)) - f(\ell, x, v) + \int_0^t \mathcal{A}f(\ell(s), x(s), v(s)) ds, \quad \forall (\ell, x, v) \in \tilde{E}$$

is a local martingale (Davis, 1993, Section 24) on \tilde{E} , then $f \circ \iota: f \in \mathcal{D}(\tilde{\mathcal{A}})$ and \mathcal{A} solve the martingale problem on E (for any local martingale Z_t on \tilde{E} , $\iota(Z_t)$ is a local martingale on E). \square

By the Feller property, the extended generator is an extension of the generator defined as

$$\mathcal{L}f(x) := \lim_{t \downarrow 0} \frac{E[f(X_t, V_t) \mid X_0 = x, V_0 = v] - f(x, v)}{t}$$

for a sufficient regular class of functions f for which this limit exists uniformly in x (see Liggett, 2010, Section 3, for more details). Then, $D = \{f \in \mathcal{D}(\mathcal{A}) : f \in C_b^1, \mathcal{A}f \in C_b(E)\}$ is a core for \mathcal{A} (as in Liggett, 2010, Definition 3.31). Let \mathcal{L} be the restriction of \mathcal{A} on D . By Liggett (2010, Theorem 3.37), μ is the unique invariant measure if, for all $f \in D$:

$$\int \mathcal{L}f d\mu = 0.$$

A.5 Remaining part of the proof

Invariant measure of the Sticky Zig-Zag process: We check here that the sticky d -dimensional Zig-Zag process as presented in Section 2.2 taking values in E with discrete velocities in $\mathcal{V} = \{v : |v_i| = a_i, \forall i \in \{1, 2, \dots, d\}\}$ and with extended generator \mathcal{A} is such that

$$\int \mathcal{L}f(x, v) \mu(dx, dv) = 0$$

for all $f \in D = \{f \in C_c^1(E), \mathcal{A}f \in C_b(E)\}$. Here, \mathcal{L} is the extended generator \mathcal{A} restricted to D (See Proposition (2.2)). For any $f \in D$, define $\lambda_i^+ := \lambda_i(x, v[i: \cdot, a_i])$, $\lambda_i^- := \lambda_i(x, v[i: \cdot, -a_i])$, $f_i^+ := f(x, v[i: a_i])$, $f_i^- := f(x, v[i: -a_i])$, $f_i^+(y) := f(x[i: y], v[i: a_i])$, $f_i^-(y) := f(x[i: y], v[i: -a_i])$. Also write the measure $\rho(dx_i, v_i) := dx_i + \frac{1}{\kappa} (\mathbb{1}_{v_i < 0} \delta_0^+(dx_i) + \mathbb{1}_{v_i > 0} \delta_0^-(dx_i))$. We see that

$$\begin{aligned} \int \mathcal{L}_i f d\mu = & \sum_{v \in \mathcal{V}^{-i}} \left(\int_{\mathbb{R}^{d-1}} \left(\int_{0^+}^{\infty} + \int_{-\infty}^{0^-} \right) (a_i \partial_{x_i} f_i^+ + \lambda_i^+ (f_i^- - f_i^+)) \exp(-\Psi(x)) dx_i \prod_{j \neq i} \rho(dx_j, v_j) \right) \\ & + \sum_{v \in \mathcal{V}^{-i}} \left(\int_{\mathbb{R}^{d-1}} \left(\int_{0^+}^{\infty} + \int_{-\infty}^{0^-} \right) (-a_i \partial_{x_i} f_i^- + \lambda_i^- (f_i^+ - f_i^-)) \exp(-\Psi(x)) dx_i \prod_{j \neq i} \rho(dx_j, v_j) \right) \\ & + \sum_{v \in \mathcal{V}^{-i}} \left(\int_{\mathbb{R}^{d-1}} a_i (f_i^+(0^+) - f_i^+(0^-)) \exp(-\Psi(x[i: 0])) \prod_{j \neq i} \rho(dx_j, v_j) \right) \\ & + \sum_{v \in \mathcal{V}^{-i}} \left(\int_{\mathbb{R}^{d-1}} -a_i (f_i^-(0^-) - f_i^-(0^+)) \exp(-\Psi(x[i: 0])) \prod_{j \neq i} \rho(dx_j, v_j) \right). \end{aligned}$$

By integration by parts we have that $\left(\int_{0^+}^{\infty} + \int_{-\infty}^{0^-} \right) (\partial_{x_i} f(x, v) \exp(-\Psi(x))) dx_i$ is equal to

$$(f(x[i: 0^-], v) - f(x[i: 0^+], v)) \exp(-\Psi(x[i: 0])) + \left(\int_{0^+}^{\infty} + \int_{-\infty}^{0^-} \right) (\partial_i \Psi(x) f(x, v) \exp(-\Psi(x))) dx_i$$

so that $\int \mathcal{L}_i f d\mu$ is equal to

$$\begin{aligned}
& \sum_{v \in \mathcal{V}^{-i}} \left(\int_{\mathbb{R}^{d-1}} \left(\int_{0^+}^{\infty} + \int_{-\infty}^{0^-} \right) (a_i \partial_{x_i} \Psi(x) + \lambda_i^+ - \lambda_i^-) f_i^- \exp(-\Psi(x)) dx_i \prod_{j \neq i} \rho(dx_j, v_j) \right) \\
& + \sum_{v \in \mathcal{V}^{-i}} \left(\int_{\mathbb{R}^{d-1}} \left(\int_{0^+}^{\infty} + \int_{-\infty}^{0^-} \right) (-a_i \partial_{x_i} \Psi(x) + \lambda_i^- - \lambda_i^+) f_i^+ \exp(-\Psi(x)) dx_i \prod_{j \neq i} \rho(dx_j, v_j) \right) \\
& + \sum_{v \in \mathcal{V}^{-i}} \left(\int_{\mathbb{R}^{d-1}} a_i (f_i^+(0^+) - f_i^+(0^-)) \exp(-\Psi(x[i: 0])) \prod_{j \neq i} \rho(dx_j, v_j) \right) \\
& + \sum_{v \in \mathcal{V}^{-i}} \left(\int_{\mathbb{R}^{d-1}} -a_i (f_i^-(0^-) - f_i^-(0^+)) \exp(-\Psi(x[i: 0])) \prod_{j \neq i} \rho(dx_j, v_j) \right) \\
& + \sum_{v \in \mathcal{V}^{-i}} \left(\int_{\mathbb{R}^{d-1}} a_i (f_i^+(0^-) - f_i^+(0^+)) \exp(-\Psi(x[i: 0])) \prod_{j \neq i} \rho(dx_j, v_j) \right) \\
& + \sum_{v \in \mathcal{V}^{-i}} \left(\int_{\mathbb{R}^{d-1}} -a_i (f_i^-(0^+) - f_i^-(0^-)) \exp(-\Psi(x[i: 0])) \prod_{j \neq i} \rho(dx_j, v_j) \right) = 0,
\end{aligned}$$

where we used that $-v_i \partial_i \Psi(x) + \lambda_i(x, v) - \lambda_i(x, F_i(v)) = 0$, $\forall (x, v) \in E$.

B Other sticky PDMP samplers

Here we extend the results presented in Section 2.2 for two other Sticky PDMP samplers: the sticky version of the Bouncy particle sampler (Bouchard-Côté, Vollmer, and Doucet, 2018) and the Boomerang sampler (Bierkens et al., 2020), the latter having Hamiltonian deterministic dynamics invariant to a prescribed Gaussian measure. To visually assess the difference in sample paths, we show in Figure 11 a typical realization of the Sticky Zig-Zag sampler, Sticky Bouncy particle sampler and Sticky Boomerang sampler.

B.1 Sticky Bouncy Particle sampler

The inner product and the norm operator in the subspace determined by A is denoted by $\langle x, v \rangle_A := \sum_{i \in A} x_i v_i$ and $\|x\|_A := \sum_{i \in A} x_i^2$ with the convention that $\langle \cdot, \cdot \rangle_{\{1, 2, \dots, d\}} = \langle \cdot, \cdot \rangle$ and $\|\cdot\|_{\{1, 2, \dots, d\}} = \|\cdot\|$. The deterministic dynamics of the sticky Bouncy Particle process are identical to that of the Sticky Zig-Zag process, having piecewise constant velocity. For each $i \in \{1, 2, \dots, d\}$, when the process hits a state $(x, v) \in \mathfrak{F}_i$, the i th coordinate (x_i, v_i) sticks for an exponentially distributed time with rate equal to $\kappa_i |v_i|$ while the other coordinates continue their flow until a reflection or refreshment event happens. A reflection occurs with an inhomogeneous rate equal to

$$\lambda(x, v) = \max(0, \langle v, \nabla \Psi(x) \rangle_\alpha),$$

where α is as defined in Equation (2.1). At reflection time the process jumps with a contour reflection of the active velocities with respect to $\nabla \Psi$:

$$(R_\Psi(x, v)v)_i = \begin{cases} v_i & i \notin \alpha(x, v) \\ v_i - 2 \frac{\langle \nabla \Psi(x), v \rangle_\alpha}{\|\nabla \Psi(x)\|_\alpha^2} \partial_i \Psi(x) & \text{else.} \end{cases}$$

Similarly to the ordinary Bouncy Particle sampler, the sticky Bouncy Particle sampler refreshes its velocity component at exponentially distributed times with homogeneous rate equal to λ_{ref} . This is

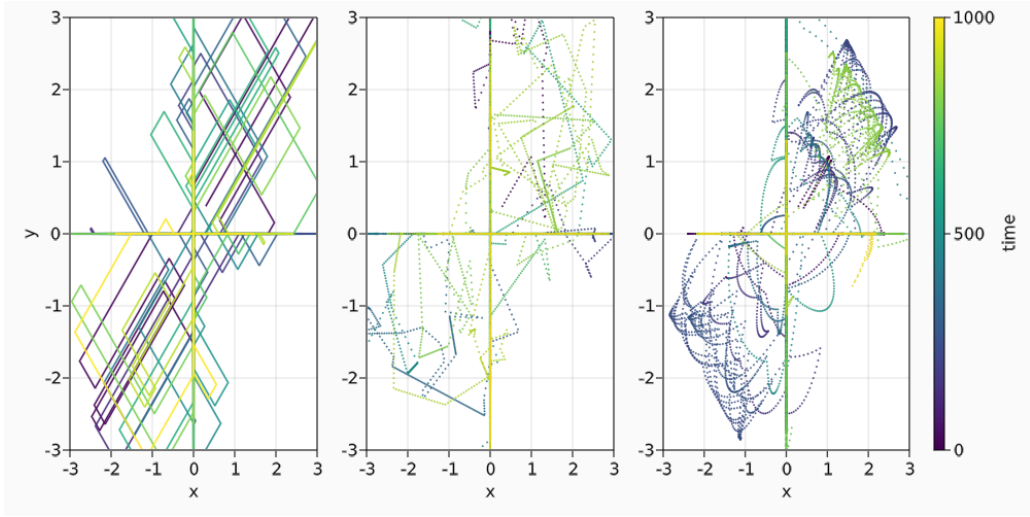


FIGURE 11: $(x-y)$ phase portraits, of 3 different sticky PDMP samplers targeting the measure of equation (1.2) with $\exp(-\Psi)$ being a mixture of two bivariate Gaussian densities centered respectively in the first and the third quadrant of the $x-y$ axes. Left: Sticky Zig-Zag sampler. Middle: sticky Bouncy Particle sampler with refreshment rate equal to 0.1. Right: sticky Boomerang sampler with refreshment rate equal to 0.1. For all the samplers, $\kappa_1 = \kappa_2 = 0.1$ and the final clock was set to $T = 10^3$. As the sticky Bouncy Particle sampler and the Boomerang sampler don't have constant speed, we marked their continuous trajectories in the phase plots with dots. The distance of dots indicates the speed of traversal.

necessary for avoiding pathological behaviour of the process (see Bouchard-Côté, Vollmer, and Doucet, 2018). At refreshment times, each coordinate renews its velocity component independently according to the following refreshment rule

$$v'_i \sim \begin{cases} Z_i & (x, v) \notin \mathfrak{F}_i, \\ \text{sign}(v_i)|Z_i| & (x, v) \in \mathfrak{F}_i, \end{cases} \quad (\text{B.1})$$

where $Z_i \stackrel{i.i.d.}{\sim} \mathcal{N}(0, 1)$, independently of all random quantities. The refreshment rule coincides with the refreshment rule given in the ordinary Bouncy Particle sampler algorithm Bouchard-Côté, Vollmer, and Doucet (2018) for the coordinates whose index is in the set α . For the components which are stuck at 0, the refreshment rule renews the velocity without changing its sign. This prevents the possibility for the i th stuck component to jump out the set \mathfrak{F}_i (changing its label from frozen to active at refreshment time).

The extended generator of the sticky Bouncy Particle sampler is given by

$$\mathcal{A}f(x, v) = \sum_{i=1}^d \mathcal{G}_i f(x, v) + \lambda(x, v)(f(x, R_\Psi(x, v)v) - f(x, v)) + \lambda_{\text{ref}} \int (f(x, w) - f(x, v)) \varrho_{x, v}(w) dw$$

and

$$\mathcal{G}_i f(x, v) = \begin{cases} |v_i| \kappa_i (f(T_i(x, v)) - f(x, v)) & (x, v) \in \mathfrak{F}_i \\ v_i \partial_{x_i} f(x, v) & \text{else,} \end{cases}$$

where

$$\varrho_{x, v}(w) = \rho(w_{\alpha(x, v)}) \prod_{i \in \alpha(x, v)^c} 2\rho(w_i) \mathbb{1}_{v_i w_i > 0},$$

for sufficient regular functions $f: E \rightarrow \mathbb{R}$ in the extended domain of the generator. Here, $\rho(y)$ is the standard normal density function evaluated at y .

Proposition B.1. *The d -dimensional sticky Bouncy Particle sampler is invariant to the measure*

$$\mu(dx, dv) = \frac{1}{C} \exp(-\Psi(x)) \prod_{i=1}^d \left(dx_i + \frac{1}{\kappa_i} (\mathbb{1}_{v_i > 0} \delta_{0^-}(dx_i) + \mathbb{1}_{v_i < 0} \delta_{0^+}(dx_i)) \rho(v) dv \right) \quad (\text{B.2})$$

for some normalization constant C .

Proof. The transition kernel $R_\Psi(x)$ satisfies the following properties:

$$\langle \nabla \Psi(x), R_\Psi(x, v)v \rangle_\alpha = -\langle \nabla \Psi(x), v \rangle_\alpha$$

and

$$\|R_\Psi(x, v)v\|^2 = \|v\|_{\alpha^c}^2 + \|R_\Psi(x, v)v\|_\alpha^2 = \|v\|_{\alpha^c}^2 + \|v\|_\alpha^2 = \|v\|^2$$

so, $\rho(R_\Psi^A(x)v) = \rho(v)$ ($\rho(x)$ here denotes the standard Gaussian density evaluated at x). Furthermore λ satisfies

$$-\langle v, \nabla \Psi(x) \rangle_\alpha + \lambda(x, v) - \lambda(x, R_\Psi(x, v)v) = 0, \quad \forall (x, v) \in E. \quad (\text{B.3})$$

Let us check that the process satisfies $\int \mathcal{L}f(x, v)\mu(dx, dv) = 0$, for all $f \in D = \{f \in C_c^1(E), \mathcal{A}f \in C_b(E)\}$ where \mathcal{L} is the extended generator \mathcal{A} restricted to D .

First let us fix some notation: denote $f_i(y) = f(x[i: y], v)$, $Rf(x, v) = f(x, R_\Psi(x, v)v)$ and $R\lambda(x, v) = \lambda(x, R_\Psi(x, v)v)$. Also write $\delta_0(dx_i, v_i) := \mathbb{1}_{v_i < 0} \delta_{0^+}(dx_i) + \mathbb{1}_{v_i > 0} \delta_{0^-}(dx_i)$ and $\Delta_i f(x, v) := f(x[i: 0^+], v) - f(x[i: 0^-], v)$. We have this preliminary result:

$$\begin{aligned} \int \sum_{i=1}^d \mathcal{G}_i f d\mu &= \frac{1}{C} \sum_i \int \left(\mathcal{G}_i f \exp(-\Psi(x)) (dx_i + \frac{1}{\kappa_i} \delta_0(dx_i)) \right) \prod_{j \neq i} \left(dx_j + \frac{1}{\kappa_j} \delta_0(dx_j, v_j) \right) \rho(v) dv \\ &= \frac{1}{C} \sum_i \int (v_i \partial_{x_i} f \exp(-\Psi(x)) dx_i + v_i \Delta_i f \exp(-\Psi(x)) \delta_0(dx_i)) \prod_{j \neq i} \left(dx_j + \frac{1}{\kappa_j} \delta_0(dx_j, v_j) \right) \rho(v) dv \end{aligned} \quad (\text{B.4})$$

$$= \frac{1}{C} \sum_i \int (v_i \partial_{x_i} \Psi(x) f(x, v) \exp(-\Psi(x)) dx_i) \prod_{j \neq i} \left(dx_j + \frac{1}{\kappa_j} \delta_0(dx_j, v_j) \right) \rho(v) dv \quad (\text{B.5})$$

$$= \frac{1}{C} \sum_{A \subset \{1, \dots, d\}} \left(\sum_{i \in A} \left(\int v_i \partial_{x_i} \Psi(x) f(x, v) \exp(-\Psi(x)) dx_A \right) \prod_{j \in A^c} \frac{1}{\kappa_j} \delta_0(dx_j, v_j) \right) \quad (\text{B.6})$$

$$= \frac{1}{C} \sum_{A \subset \{1, \dots, d\}} \int \langle v, \nabla \Psi(x[A^c: 0]) \rangle_{\mathcal{A}} f(x[A^c: 0], v) \exp(-\Psi(x[A^c: 0])) dx_A \prod_{j \in A^c} \frac{1}{\kappa_j} \rho(v) dv$$

Here from (B.4) to (B.5) we used integration by parts in the two half planes $(\infty, 0^+]$ and $[0^-, -\infty)$. For the equivalence of (B.5) to (B.6) note that placing $|A|$ balls in d numbered boxes and marking one of them (say the ball in box i) is equivalent to placing a marked ball in box i and distributing the remaining unmarked balls over the remaining boxes. Also notice that

$$\begin{aligned} \int \lambda_{\text{ref}} \int f(x, w) - f(x, v) \varrho(w) dw d\mu &= \\ \frac{1}{C} \sum_{A \subset \{1, 2, \dots, d\}} \lambda_{\text{ref}} \int (f(x, w) - f(x, v)) \exp(-\Psi(x)) dx_A & \\ \times \prod_{i \in A^c} \frac{1}{\kappa_i} \delta_{0^-}(dx_i) \mathbb{1}_{v_i > 0} \mathbb{1}_{w_i > 0} 2^{|A^c|} \rho(v) \rho(w) dv dw & \\ + \frac{1}{C} \sum_{A \subset \{1, 2, \dots, d\}} \lambda_{\text{ref}} \int (f(x, w) - f(x, v)) \exp(-\Psi(x)) dx_A & \\ \times \prod_{i \in A^c} \frac{1}{\kappa_i} \delta_{0^+}(dx_i) \mathbb{1}_{v_i < 0} \mathbb{1}_{w_i < 0} 2^{|A^c|} \rho(v) \rho(w) dv dw, & \end{aligned}$$

which is equal to 0 by symmetry between v and w . Then

$$\begin{aligned} \int \mathcal{L}f d\mu &= \frac{1}{C} \sum_{A \subset \{1, \dots, d\}} \int \langle v, \nabla \Psi(x[A^c: 0]) \rangle_A \exp(-\Psi(x[A^c: 0])) f(x[A^c: 0], v) dx_A \prod_{j \in A^c} \frac{1}{\kappa_j} \rho(v) dv \\ &\quad + \int (\lambda(x, R_\Psi(x, v)) - \lambda(x, v)) f(x, v) \mu(dx, dv) \\ &= \frac{1}{C} \sum_{A \subset \{1, \dots, d\}} \int \langle v, \nabla \Psi(x[A^c: 0]) \rangle_A \exp(-\Psi(x[A^c: 0])) f(x[A^c: 0], v) dx_A \prod_{j \in A^c} \frac{1}{\kappa_j} \rho(v) dv \end{aligned} \tag{B.7}$$

$$\begin{aligned} &+ \frac{1}{C} \sum_{A \subset \{1, \dots, d\}} \int (\lambda(x[A^c: 0], R_\Psi v) - \lambda(x[A^c: 0], v)) f(x[A^c: 0], v) \exp(-\Psi(x[A^c: 0])) dx_A \\ &\quad \times \prod_{j \in A^c} \frac{1}{\kappa_j} \rho(v) dv \\ &= 0, \end{aligned} \tag{B.8}$$

where in equations (B.7)-(B.8) we used a change of variable $v' = R_\Psi(x, v)v$ and property (B.3). \square

Remark B.2. In more generality, the transition kernel at refreshment times can be chosen as follows: with two refreshment transition densities q^A and q^F such that $q^A(w_A | v_A)\rho(v_A)$ and $q^F(w_F | v_F)\rho(v_F)$ for each $A \sqcup F = \{1, \dots, d\}$ are symmetric densities in w, v , the refreshment kernel

$$\varrho_{x,v}(dy, dw) = q^A(w_{\alpha(x,v)} | w_{\alpha(x,v)}) q^F(w_{\alpha^c(x,v)} | w_{\alpha^c(x,v)}) \delta_{\mathcal{F}(x,v,w)}(dy) dw$$

where

$$(\mathcal{F}(x, v, w))_i = \begin{cases} 0^- & \text{if } x_i = 0^+, v_i < 0, w_i > 0, \\ 0^+ & \text{if } x_i = 0^-, v_i > 0, w_i < 0, \\ x_i & \text{else} \end{cases}$$

leaves the target measure μ invariant.

The transition kernels given in Remark B.2 satisfy the equation $\lambda_{\text{ref}} \int f(x, w) - x(x, v) \varrho_{x,w} dw d\mu = 0$ and therefore, by similar computations as in the proof of Proposition B.1, leave μ invariant. For example, the preconditioned Crank-Nicolson scheme Cotter et al. (2013) falls within this setting.

B.2 Sticky Boomerang sampler

The sticky Boomerang sampler has Hamiltonian dynamics prescribed by the vector field $\xi(x_i, v_i) = (v_i, -x_i)$ with close-form solution

$$(x_i(t), v_i(t)) = (\cos(t)x_i(0) + \sin(t)v_i(0), -x_i(0)\sin(t) + \cos(t)v_i(0)), \tag{B.9}$$

and is invariant to a prescribed Gaussian measure centered in 0. Define $U(x)$ such that

$$U(x) = \Psi(x) - \frac{1}{2} x' \Sigma^{-1} x$$

for a positive semi-definite matrix $\Sigma \in \mathbb{R}^{d \times d}$. Consider for example the application in Bayesian inference with spike-and-slab prior (equation (1.1)) where $\{\pi_i\}_{i=1}^d$ are centered Gaussian densities with variance σ_i^2 . Then a natural choice is $\Sigma = \text{Diag}(\sigma_1^2, \sigma_2^2, \dots, \sigma_n^2)$.

Similarly to the sticky Bouncy Particle sampler, the process reflects its velocity at an inhomogeneous rate given by

$$\lambda(x, v) = \langle v, \nabla U(x) \rangle_\alpha^+$$

with reflection specified by the transition kernel

$$(R_U(x, v)v)_i = \begin{cases} v_i & i \notin \alpha \\ v_i - 2 \frac{\langle \nabla U(x, v) \rangle_\alpha}{\|\nabla \Sigma^{1/2} U(x)\|_\alpha^2} \langle \Sigma_{[i, :]}, \nabla U(x) \rangle_\alpha & \text{else} \end{cases}$$

and refreshes the velocity at exponentially distributed times with rate equal to λ_{ref} according to the rule given in equation (B.1).

Proposition B.3. *The d -dimensional sticky Boomerang sampler is invariant to the measure in equation (B.2).*

Proof. The extended generator of the sticky d -dimensional Boomerang process is given by

$$\mathcal{A}f(x, v) = \sum_{i=1}^d \mathcal{G}_i f(x, v) + \lambda(x, v)(f(x, R_U(x, v)v) - f(x, v)) + \lambda_{\text{ref}} \int (f(x, w) - f(x, v)) \varrho_{x, v}(w) dw$$

and

$$\mathcal{G}_i f(x, v) = \begin{cases} |v_i| \kappa_i (f(T_i(x, v)) - f(x, v)) & (x, v) \in \mathfrak{F}_i \\ v_i \partial_{x_i} f(x, v) + x_i \partial_{v_i} f(x, v) & \text{else,} \end{cases}$$

where

$$\varrho_{x, v}(w) = \rho(w_{\alpha(x, v)}) \prod_{i \in \alpha(x, v)^c} 2\rho(w_i) \mathbb{1}_{v_i w_i > 0},$$

$\rho(y)$ being the standard normal density function evaluated at y and for sufficient regular functions $f: E \rightarrow \mathbb{R}$ in the extended domain of the generator. Then, define $D = \{f \in C_c^1(E), \mathcal{A}f \in C_b(E)\}$ and \mathcal{L} as the extended generator \mathcal{A} restricted to D . The component of the extended generator $(x, v) \rightarrow \partial_{x_i} f(x, v) + x_i \partial_{v_i} f(x, v)$ produces Hamiltonian dynamics (see equation (B.9)) preserving any Gaussian measure centered on 0. Notice that the $R_U(x)$ satisfies

$$\langle \nabla U(x), R_U(x)v \rangle_{\alpha(x, v)} = -\langle \nabla U(x), v \rangle_{\alpha(x, v)}$$

and that

$$\|\Sigma^{-1/2} R_U(x)v\| = \|\Sigma^{-1/2} v\|.$$

Then one can check that $\int \mathcal{L}f(x, v) \mu(dx, dv) = 0$ by carrying out similar computations as in the proof of Proposition B.1. \square

A variant of the sticky Boomerang sampler is the sticky factorised Boomerang sampler (being the sticky version of the factorised Boomerang sampler introduced in Bierkens et al., 2020). Here the process has the same dynamics, refreshment rule and sticky events of the sticky Boomerang process but has a different reflection rate and reflection rule. Similarly to the Sticky Zig-Zag process, the first reflection time of the sticky factorised Boomerang sampler is given by the minimum of $|\alpha(x, v)|$ Poisson times $\{\tau_j: j \in \alpha(x, v)\}$ with $\tau_j \sim \text{Pois}(t \rightarrow \lambda_j(\varphi(t, x, v)))$ and $\lambda_j(x, v) = (\partial_{x_j} U(x)v_j)^+$. Likewise the Sticky Zig-Zag process, at the reflection time the process reflects its velocity by changing the sign of the i th component $v \rightarrow v[i: -v_i]$ where $i = \text{argmin}\{\tau_j: j \in \alpha(x, v)\}$. As shown in Bierkens et al. (2020) and argued briefly in Section 3, the factorised Boomerang sampler can outperform the Boomerang sampler when $\partial_{x_i} U$ is function of few coordinates (see Section 3 for the computational advantages of factorised samplers). In this section, we closely follow the general construction of piecewise deterministic processes and the main results of Davis (1993, Section 24). In order to facilitate the reading of the section, we follow the same notation of Davis (1993) so that the results derived here can be compared easily.

C Comparison between reversible jump PDMPs and sticky PDMPs

Here we investigate the possibility of introducing the parameter p to the Sticky Zig-Zag sampler. This parameter was originally introduced in Chevallier, Fearnhead, and Sutton, 2020. We also highlight the different limiting behaviour between the RJ-PDMP samplers and the sticky PDMP samplers as the number of Dirac measures increases.

Based on an heuristic argument and a simulation study, we conclude that the introduction of p does not improve the performance of the Sticky Zig-Zag sampler.

C.1 Heuristics for the choice of p

The parameter p defines the probability for a coordinate to stick at 0 when it hits 0. By introducing this parameter, the times of the particles stuck at 0 has to be rescaled by a factor of p in order target the right measure. The parameter p was originally introduced in Chevallier, Fearnhead, and Sutton, 2020.

Consider a trajectory $\{z_t: 0 < t < T\}$ of the one dimensional ordinary Zig-Zag sampler (without stickiness) targeting a given measure. In this case, one could create a trajectory of the Sticky Zig-Zag process retrospectively just by adding constant segments equal to 0, every time the process hits 0 with random length equal to XY , with $X \sim \text{Ber}(p)$ and $Y \sim \text{Exp}(\kappa/p)$, X independent from Y . Then, if the trajectory z_t hits 0 N -times, the total occupation time of the sticky process in 0 is Gamma-distributed with shape parameters $\frac{N}{p}$ and inverse scale parameter $p\kappa$ (in variable selection, this would correspond to the posterior probability of the sub-model without the coefficient). While the mean of this random variable is constant for every p , its variance is $\frac{N}{\kappa p}$ and is minimized when $p = 1$.

Based on the aforementioned heuristics, it appears not useful to introduce the parameter p for the Sticky Zig-Zag. This claim is supported by simulations presented in Figure 12, where we vary p from 0.1 (top) to 1.0 (bottom) for a 20 dimensional Gaussian density with pairwise correlation equal to 0.99 and relative to the measure

$$\prod_{i=1}^d (dx_i + c \sum_{j \in \mathbb{N}} \delta_{j \neq 0.01}(dx_i)), \quad (\text{C.1})$$

with $c = 1.0$. In Figure 12, left panels, the traces are more erratic when p is small and the traverses the space is less time when p is large (notice the different ranges of the vertical axis). In Figure 12, right panels, the phase portrait of the first two coordinates is shown. By visual inspection it is possible to notice that the phase portrait fails to be symmetric on the axis $x_1 = -x_2$ for p small while it succeeds for $p = 1$ (notice again the different ranges of the axes), hence suggesting that Zig-Zag sampler has a better mixing for $p = 1$.

C.2 Limiting behaviour

As the number of Dirac measures increases, the behaviour of the Sticky Zig-Zag and the RJ Zig-Zag sampler differ significantly. This is because after every time a coordinate sticks at a point mass, the former sampler preserves the velocity component while the latter sampler has to refresh a new independent velocity. We illustrate the limiting behaviour of the two samplers through simulations where we let the Sticky Zig-Zag and the RJ-Zig-Zag sampler (with $p = 0.6$) target a 20-dimensional measure with a Gaussian density with pairwise correlation equal to 0 (Figure 13) and 0.99 (Figure 14) relative to the reference measure of equation (C.1) with $c = 10$. While the Sticky Zig-Zag sampler resemble an ordinary Zig-Zag sampler, the RJ-PDMP sampler has a limiting diffusive behaviour and appears to explore the space less efficiently than the sticky PDMP sampler (see the range of the axes and the symmetries of the measure around the axis $x_2 = -x_1$).

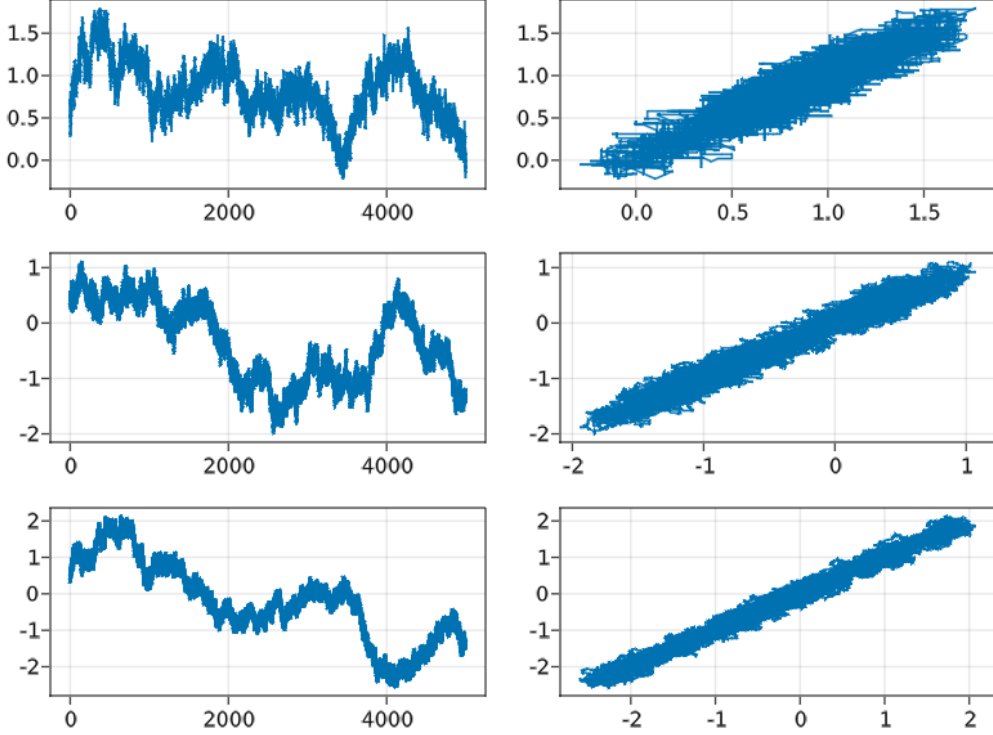


FIGURE 12: x_1 trace plots (left) and x_1 - x_2 phase portraits (right) of the Sticky Zig-Zag samplers with final clock $T = 50^3$ with p equal to 0.1 (top), 0.5 (center), 1.0 (bottom). The target measure has a Gaussian density with pairwise correlation equal to 0.99 relative to the reference measure of equation (C.1). By comparing the symmetry of the empirical measures along the diagonal and the range of the coordinates, one can conclude that the algorithm performs best for $p = 1$.

D Details of Section 4 and Section 5

D.1 Bayes factors for Gaussian models

Let $(X, Y) \sim N(\mu, \Gamma^{-1})$, written in block form as

$$\mu = \begin{bmatrix} \mu_x \\ \mu_y \end{bmatrix}, \quad \Gamma = \begin{bmatrix} \Gamma_x & \Gamma_{xy} \\ \Gamma'_{xy} & \Gamma_y \end{bmatrix}.$$

Denote the density of (X, Y) evaluated at (x, y) by $\phi([x, y]; \mu, \Gamma^{-1})$.

Lemma D.1. (Conditional density)

$$X \mid (Y = y) \sim N(\mu_{x|y}, \Gamma_x)$$

where $\mu_{x|y} = \mu_x - \Gamma_x^{-1} \Gamma_{xy}(y - \mu_y)$

Lemma D.2. (Marginal density) Assume Γ_x to be positive definite, then

$$\int \phi([x, y]; \mu, \Gamma^{-1}) dx = (2\pi)^{\frac{d_x-d}{2}} |\Gamma|^{\frac{1}{2}} |\Gamma_x|^{-\frac{1}{2}} \exp\left(\frac{1}{2} \mu'_{x|y} \Gamma_x \mu_{x|y} - \frac{1}{2} [-\mu_x, y - \mu_y]' \Gamma [-\mu_x, y - \mu_y]\right)$$

where d_x is the size of X .

We are now ready to compute the corresponding Bayes factors of two neighbouring (sub-)models as in equation (4.1) when Ψ is a quadratic function. For every set of indexes $\alpha \subset \{1, 2, \dots, d\}$ and for every

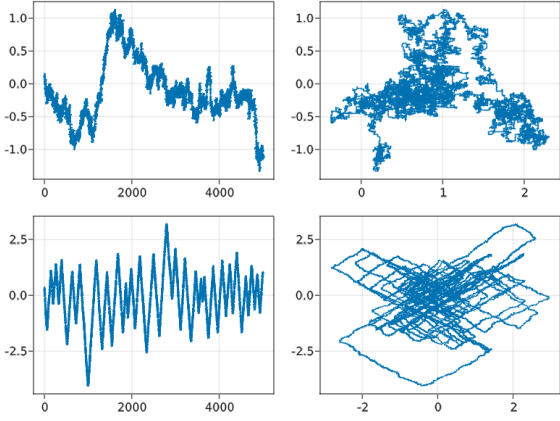


FIGURE 13: Comparison between RJ Zig-Zag samplers (first row) and Sticky Zig-Zag samplers (second row) targeting a 20 dimensional measure with Gaussian density with pairwise correlation equal to 0.0 and (columns 3 and 4) relative to the reference measure in equation (C.1). Column 1: trace plot of the first coordinate. Column 2: trace plot of the second column. In all cases $T = 10^4$. By looking at the range of each coordinate, it is clear that the Sticky Zig-Zag mixes faster than its reversible counterpart.

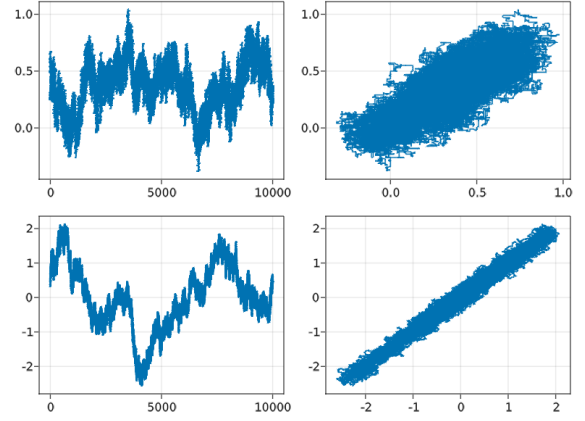


FIGURE 14: Same description as in Figure 13, except now for a Gaussian measure with pairwise correlation equal to 0.99. By looking for example at the symmetry along the axis $x_2 = -x_1$ and the ranges of the coordinates, it is clear that the Sticky Zig-Zag outperforms the RJ Zig-Zag.

j , the Bayes factors relative to two neighbouring (sub-)models (those differing by only one coefficient) for a measure as in equation (1.2) are given by

$$B_j(\alpha) = \frac{\mu(\mathcal{M}_{\alpha \cup \{j\}})}{\mu(\mathcal{M}_{\alpha \setminus \{j\}})} = \frac{\kappa_i \int_{\mathbb{R}^{|\alpha \cup \{j\}|}} \exp(-\Psi(y)) dx_{\alpha \cup \{j\}}}{\int_{\mathbb{R}^{|\alpha \setminus \{j\}|}} \exp(-\Psi(z)) dx_{\alpha \setminus \{j\}}}, \quad (\text{D.1})$$

where $y = \{x \in \mathbb{R}^d : x_i = 0, i \notin (\alpha \cup \{j\})\}$, $z = \{x \in \mathbb{R}^d : x_i = 0, i \notin (\alpha \setminus \{j\})\}$. Since Ψ is quadratic, we can write $\exp(-\Psi(x)) = C\phi(x, \mu, \Gamma^{-1})$ for some parameters C, μ, Γ . By using both Lemma D.1 and Lemma D.2 we have that the right hand side of equation (D.1) is equal to

$$\kappa_i \sqrt{\frac{2\pi|\Gamma_{x_1}|}{|\Gamma_{x_2}|}} \exp\left(\frac{1}{2}(\mu'_{x_1|y_1=\mathbf{0}} \Gamma_{x_1} \mu_{x_1|y_1=\mathbf{0}} - \mu'_{x_2|y_2=\mathbf{0}} \Gamma_{x_2} \mu_{x_2|y_2=\mathbf{0}})\right)$$

where $x_1 = x_{\alpha_{-j} \cup \{j\}}$, $x_2 = x_{\alpha_{-j} \setminus \{j\}}$, $y_1 = x_{\alpha_{-j}^c \setminus \{j\}}$, $y_2 = x_{\alpha_{-j}^c \cup \{j\}}$. Furthermore, by Lemma D.1, the random variable at step 2 of the Gibbs sampler presented in Section 4.1 can be simulated as $X_\alpha | (X_{\alpha^c} = \mathbf{0}) \sim \mathcal{N}(\mu_{x_\alpha | x_{\alpha^c} = \mathbf{0}}, \Gamma_{x_\alpha})$.

D.2 Logistic regression

Similar computations for the bounds of the Poisson rates of the Zig-Zag sampler applied to logistic regressions can be found in the supplementary material of Bierkens, Fearnhead, and Roberts (2019). Given a posterior density of the form of equation (1.2) with

$$\Psi(x) = \sum_{j=1}^N \left(\log \left(1 + e^{\langle A_{[j,:], x} \rangle} \right) - y_j \langle A_{[j,:], x} \rangle \right) + \frac{1}{2\sigma^2} \|x\|^2$$

we use the Sticky Zig-Zag subsampler presented in Section 2.3. To that end, define $U(x) = \Psi(x) - \frac{1}{2\sigma^2}\|x\|^2$. We decompose the partial derivatives of U as follow:

$$\partial_{x_i}U(x) = \sum_{j \in \Gamma_i} S(x, i, j)$$

with sets $\Gamma_i = \{j \in \{1, 2, \dots, N\} : A_{j,i} \neq 0\}$ and

$$S(x, i, j) = \left(\frac{A_{[j,i]} e^{\langle A_{[j,i]}, x \rangle}}{1 + e^{\langle A_{[j,i]}, x \rangle}} - y_j A_{[j,i]} \right).$$

Then, for all $i = 1, 2, \dots, p$ and any $x' \in \mathbb{R}^p$, if $J \sim \text{Unif}(\Gamma_k)$, the estimator $[|\Gamma_i|(S(x, i, J) - S(x', i, J))] + \partial_{x_i}U(x^*) + \sigma^{-2}x_i$ is unbiased for $\partial_{x_i}\Psi(x)$. Notice that the partial derivative of $S(x, k, j)$ is bounded:

$$\partial_{x_i}(S(x, k, j)) = \frac{A_{[j,k]}A_{[j,i]}e^{\langle A_{[j,i]}, x \rangle}}{(1 + e^{\langle A_{[j,i]}, x \rangle})^2} \leq \frac{1}{4}A_{[j,k]}A_{[j,i]},$$

which means that for $i = 1, 2, \dots, d$

$$|S(x, i, j) - S(x', i, j)| \leq C_i \|x - x'\|_p, \quad p \geq 1, j \in \Gamma_i, x, x' \in \mathbb{R}^d,$$

with

$$C_k = \frac{1}{4} \max_{j=1, \dots, N} |A_{[j,k]}| \|A_{j,\cdot}\|_2.$$

Then given an initial position $(x, v) \in E$, tuning parameter x' and for any $t \geq 0$, write $(x(t), v(t)) = \varphi(t, x, v)$ with $i \in \alpha(x, v)$:

$$\begin{aligned} \tilde{\lambda}_i(x(t), v(t)) &= (v_i (\partial_{x_i}U(x') + \sigma^{-2}x_i(t) + |\Gamma_i|(S(x(t), i, j) - S(x', i, j))))^+ \\ &\leq (v_i (\partial_{x_i}U(x') + \sigma^{-2}(x_i + v_i t)))^+ + |v_i| |\Gamma_i| (|S(x(t), i, j) - S(x, i, j)| + |S(x, i, j) - S(x', i, j)|) \\ &\leq (v_i (\partial_{x_i}U(x') + \sigma^{-2}(x_i + v_i t)))^+ + |v_i| |\Gamma_i| C_i (t \|v\|_p + \|x - x'\|_p). \end{aligned}$$

Thus we set

$$\lambda_i(t, x, v) = v_i(a_i(x, v) + b_i(x, v)t)$$

where $a_i(x, v) = (v_i(\partial_{x_i}U(x') + \sigma^{-2}x_i))^+ + C_i|\Gamma_i||v_i|\|x - x'\|_p$ and $b_i(x, v) = |v_i|C_i|\Gamma_i|\|v\|_p + v_i^2\sigma^{-2}$. We choose x' to be the posterior mode of $\exp(-\Psi)$, which in this case is unique and easily found with the Newton's method since the function $\exp(-\Psi)$ is convex. Given an initial position (x, v) , suppose the particle $j \neq i$ gets frozen at time $\tau \geq 0$. Then for $t \geq \tau$ we have that $\|\int_0^t v(t)dt\|_p = \tau\|v\|_p + (t - \tau)\|v'\|_p \leq t\|v\|_p$, with $v' = v[j : 0]$. This implies that the Poisson times drawn before the j th coordinate gets stuck are still valid upper bounds after time τ . The same argument follows easily for $n \geq 1$ coordinates getting stuck at 0.

D.3 Spatially structured sparsity

For this application, we use the thinning scheme as presented in Section 3.1. The bounding rates are of the form

$$\bar{\lambda}_i(t, x(t_0), v(t_0)) = (c + v_i(t_0)\partial_{x_i}\Psi(x(t_0)))^+ \tag{D.2}$$

for $t \in [0, \Delta]$ with $\Delta = 1/c$. To see this, define the Lipschitz growth bound $L_{x,v,\Delta}$ as

$$P\left(\sup_{0 < t < \Delta} \frac{1}{t} |V_i(t)\partial_{x_i}\Psi(X(t))| \leq L_{x,\Delta} \mid X(0) = 0, V(0) = v\right) = 1, \quad i = 1, 2, \dots, d,$$

which gives an explicit expression for c in equation (D.2) as

$$c - L_{\Delta}\Delta = 0 \Rightarrow \Delta = 1/c,$$

such that the inequality (3.2) holds. With $L_\Delta = \sup_x L_{x,v,\Delta}$, in this application we have that

$$L_\Delta = \sup_{v,t} |\partial_t \partial_{x_i} \Psi(x + tv)| = c_2 + 8c_1 + 1/\sigma^2$$

with c_1, c_2 defined in Section 5.2. With this given choice, in the simulations of Section 5.2, the ratio between the accepted reflection times and the proposed reflection times was 0.357. Here we used the local implementation of the Sticky Zig-Zag given by Subsection 3.2 (with sets $\bar{A}_i = i$ for all i) in conjunction with the sparse algorithm as in Remark 3.1.

D.4 Sparse precision matrix

By write $\Psi(x) \otimes_{i=1}^p \otimes_{j=1}^i (dx_{i,j} + \frac{1}{\kappa} \delta_0(dx_{i,j}) \mathbf{1}_{(i \neq j)})$ and we have that

$$\partial_{x_{i,j}} \Psi(x) = (YY')_{(i,:)} X_{(:,j)} + \gamma_{i,j}(x_{i,j} - c_{i,j}) - \mathbf{1}_{(i=j)} \left(\frac{N}{x_{i,j}} \right). \quad (\text{D.3})$$

Note that, for any initial position and velocity (x, v) , the reflection times of the Sticky Zig-Zag with rates $\lambda_{i,j}(\phi(t, x, v)) = (v_i \partial_{x_{i,j}} \Psi(x + vt))^+$ can be computed exactly for the off-diagonal elements and via a thinning scheme for the diagonal elements where

$$\lambda_{i,i}(\phi(t, x, v)) \leq \bar{\lambda}_{i,i}(t, x, v) + \bar{\bar{\lambda}}_{i,i}(t, x, v), \quad t > 0, \forall i.$$

Here $\bar{\lambda}_{i,i}(t, x, v) = (v_{i,i} (YY'_{i,:} (X_{:,i} + vt) + \gamma_{i,i}(x_{i,i} + vt - c_{i,i})))^+$ and $\bar{\bar{\lambda}}_{i,i}(t, x, v) = \left(-v_{i,i} \frac{N}{x_{i,i} + v_{i,i}t} \right)$ and a Poisson time from the bounding rate is simulated as $\min(\tau_1, \tau_2)$ where $\tau_1 \sim \text{Pois}(s \rightarrow \bar{\lambda}_{i,i}(s, x, v))$ and $\tau_2 \sim \text{Pois}(s \rightarrow \bar{\bar{\lambda}}_{i,i}(s, x, v))$.